



# Robust Flux Reconstruction and a Posteriori Error Analysis for an Elliptic Problem with Discontinuous Coefficients

Daniela Capatina, Aimene Gouasmi, Cuiyu He

## ► To cite this version:

Daniela Capatina, Aimene Gouasmi, Cuiyu He. Robust Flux Reconstruction and a Posteriori Error Analysis for an Elliptic Problem with Discontinuous Coefficients. *Journal of Scientific Computing*, 2023, 98 (1), pp.28. 10.1007/s10915-023-02428-7 . hal-04455830

**HAL Id: hal-04455830**

**<https://hal.science/hal-04455830>**

Submitted on 4 Mar 2024

**HAL** is a multi-disciplinary open access archive for the deposit and dissemination of scientific research documents, whether they are published or not. The documents may come from teaching and research institutions in France or abroad, or from public or private research centers.

L'archive ouverte pluridisciplinaire **HAL**, est destinée au dépôt et à la diffusion de documents scientifiques de niveau recherche, publiés ou non, émanant des établissements d'enseignement et de recherche français ou étrangers, des laboratoires publics ou privés.

# ROBUST FLUX RECONSTRUCTION AND A POSTERIORI ERROR ANALYSIS FOR AN ELLIPTIC PROBLEM WITH DISCONTINUOUS COEFFICIENTS

DANIELA CAPATINA <sup>\*</sup>, AIMENE GOUASMI <sup>†</sup>, AND CUIYU HE<sup>‡</sup>

**Key words.** conforming and nonconforming finite elements, discontinuous coefficients, flux recovery, *a posteriori* error estimation, adaptive mesh refinement

**AMS subject classifications.** 65N12, 65N15, 65N30

**Abstract.** In this paper, we locally construct a conservative flux for finite element solutions of elliptic interface problems with discontinuous coefficients. Since the Discontinuous Galerkin method has built-in conservative flux, we consider in this paper the conforming Finite Element Method and a special type of nonconforming method with arbitrary orders. We also perform our analysis based on Nitsche's method, which imposes the Dirichlet boundary condition weakly. The construction method is derived based on a mixed problem with one solution coinciding with the finite element solution and with the other solution being naturally used to obtain a conservative flux. We then apply the recovered flux to the *a posteriori* error estimation and prove the robust reliability and efficiency for conforming elements. Numerical experiments are provided to verify the theoretical results.

**1. Introduction.** Numerous studies have been conducted to explore the post-processing of conservative fluxes for various purposes, including *a posteriori* error estimation [1, 2], flux conservation in fluid dynamics [3], and super-convergence [4], among others [5, 6, 7, 8, 9, 10]. This paper focuses on designing a locally conservative flux in the  $H(\text{div})$  conforming Raviart-Thomas space for finite element solutions of elliptic interface problems, including both conforming and nonconforming approximations with arbitrary polynomial degree  $k \in \mathbb{N}^*$ . The recovered flux is then applied and analyzed in *a posteriori* error estimation, which plays a crucial role in adaptive methods.

Equilibrated *a posteriori* error estimators have attracted much interest due to the guaranteed reliability bound with the reliability constant equal to one. This property implies that they are perfect for discretization error control on both coarse and fine meshes. It is important to note that error control on coarse meshes is important but difficult for computationally challenging problems.

For the conforming finite element approximation, a mathematical foundation of equilibrated estimators is the Prager-Synge identity [11]. Based on this identity, various equilibrated estimators have been studied by many researchers (see, e.g., [1, 12, 13, 14, 2, 15, 16, 17, 18, 6, 19, 8, 10, 3, 20, 9]). The key ingredient for continuous finite elements is a recovered equilibrated (locally conservative) flux in the  $H(\text{div}; \Omega)$  space based on the numerical flux which is typically neither in the  $H(\text{div}; \Omega)$  space nor locally conservative. Using a partition of unity, Ladevèze and Leguillon [1] initiated a local procedure to reduce the construction of an equilibrated flux to vertex patch-based local calculations. For the continuous linear finite element approximation to the Poisson equation in two dimensions, an equilibrated flux in the lowest order Raviart-Thomas space was explicitly constructed in [18]. This explicit approach does not

<sup>\*</sup>LMAP & CNRS UMR 5142, University of Pau and Pays de l'Adour, IPRA BP 1155, 64013 Pau, France (daniela.capatina@univ-pau.fr)

<sup>†</sup>LMAP & CNRS UMR 5142, University of Pau and Pays de l'Adour, IPRA BP 1155, 64013 Pau, France (aimene.gouasmi@univ-pau.fr)

<sup>‡</sup>Department of Mathematics, Oklahoma State University, Stillwater, OK, USA, 74078 (cuiyu.he@okstate.edu)

lead to a robust equilibrated estimator with respect to the coefficient jump without introducing a constraint minimization (see [8]). The constraint minimization on each vertex-based patch may be solved by first computing an equilibrated flux and then calculating a divergence-free correction, see [20] and references therein. In [9], a unified method also based on the partition of unity was developed. This method requires solving local mixed problems on a vertex patch for each vertex. In [16, 3] a global problem is solved on the enriched piecewise constant DG space to obtain the conservative flux, which is relatively more computationally expensive.

Partition of unity is a commonly used tool for localization. In principle, it can be uniformly applied to various finite element methods. However, it is studied mainly for the continuous Galerkin method since explicit recovery for its solution has been a challenging research topic due to the continuity of the finite element space. Existing methods using partition of unity are relatively complex since it requires solving star-patched local problems that are either constrained [8] or in a mixed form [9].

For an exception apart from the partition of unity, we refer to [10] where two-dimensional Poisson problems are studied. This method is based on a unified mixed problem equivalent to conforming, nonconforming and discontinuous Galerkin methods. The idea is to use the Lagrange multiplier, defined on the facets of the mesh, as a correction of the degrees of freedom of the flux. The choice of the multiplier's space is fundamental since it should satisfy the uniform inf-sup condition and enable local construction. With this approach, one only needs to solve an explicit low-dimensional linear system for each vertex. It has recently been extended to unfitted methods [21].

In this study, we adopt a similar approach for the diffusion problem where the diffusion coefficients may undergo large jumps along the interfaces. As a result, the auxiliary mixed formulation and the local construction of its Lagrange multiplier resemble those in [10]. Our main contribution is to achieve robustness concerning the discontinuous coefficients by properly designing the algorithm and analysis.

Firstly, we consider the conforming finite element method, which is the most difficult case for the flux reconstruction. We use triangular meshes and Nitsche's method to treat the Dirichlet boundary conditions; note that in [10], the Dirichlet condition was treated strongly. We provide a well-posed equivalent mixed formulation, where the continuity of the solution and of the test-functions across the interior sides of the mesh is imposed weakly. We obtained the robust inf-sup constant in terms of the coefficients, and we establish a local bound for the multiplier (and hence, for the recovered flux) with a constant whose dependence on the coefficients is given explicitly. This type of result is new, at the best of our knowledge; for quasi-monotone coefficients, we retrieve the robustness already known in the literature for other reconstructions in this case.

Secondly, we consider a nonconforming finite element approximation of arbitrary polynomial degree  $k \in \mathbb{N}^*$ , based on the space introduced by Matthies and Tobiska [22]. The standard nonconforming space of odd degree rises with no particular difficulty, and the reconstruction of conservative fluxes, in this case, is well-known in the literature. Meanwhile, this is no longer true for an even degree  $k$ , due to the loss of insolvency cf. [23]. The main advantages of the finite elements proposed in [22] are that they are uniformly defined for any  $k$  and are also inf-sup stable for the Stokes problem. Our contribution consists in extending the approach of [10] to these spaces in a completely robust way with respect to the diffusion coefficients. To our knowledge, flux reconstruction for this type of nonconforming finite element is new.

An important use of flux recovery is in the estimation of a posteriori errors, where

the weighted  $L_2$ -norm of the difference between the numerical flux and the recovered flux can be employed. This technique is particularly valuable in adaptive mesh refinement procedures, commonly employed for problems with singularities, discontinuities, or sharp derivatives. The study of a posteriori error estimation has been an active area of research for several decades, as demonstrated by the extensive literature on the topic (see, for example, [2, 24, 7]).

In this paper, we carry out the a posteriori error analysis for the conforming case, tracking the dependence of the constants involved in the error bounds on the diffusion coefficients. We establish the sharp reliability of the a posteriori error indicator and its robust local efficiency in the case of quasi-monotone coefficients. Finally, we present several numerical experiments illustrating the theoretical results for a piecewise linear continuous method.

The paper is organized as follows. In Section 2, we give the model problem and its weak formulation. We present in Section 3 the conforming and nonconforming finite element approximations and their equivalent mixed formulations, for which we establish the well-posedness. For both discretizations, the local computation and robust bound of the multipliers are detailed in Section 4, whereas the definition of the conservative fluxes is given in Section 5. Section 6 deals with the a posteriori error estimation for the conforming approximation by means of the recovered flux. Finally, Section 7 is devoted to the numerical tests, while in the Appendix we give the proof of the inf-sup condition for the conforming method.

**Data Availability.** No data is available. Enquiries about the code should be directed to the authors.

**Ethics declaration.** The authors declare that they have no conflict of interest.

**2. Model problem and notation.** Let  $\Omega$  be a bounded domain of  $\mathbb{R}^2$  with polygonal boundary  $\partial\Omega$  with exterior unit normal  $n$ . Let  $\partial\Omega = \Gamma_D \cup \Gamma_N$ , where  $\Gamma_D$  and  $\Gamma_N$  are disjoint and, for the sake of simplicity,  $|\Gamma_D| > 0$ . We consider the following model problem: find  $u : \Omega \rightarrow \mathbb{R}$  such that

$$\begin{aligned} -\operatorname{div}(K\nabla u) &= f && \text{in } \Omega \\ u &= g_D && \text{on } \Gamma_D \\ K\nabla u \cdot n &= g_N && \text{on } \Gamma_N. \end{aligned} \tag{2.1}$$

Assume that  $f \in L^2(\Omega)$ ,  $g_N \in L^2(\Gamma_N)$ ,  $g_D \in H^{1/2}(\Gamma_D)$  and that  $K$  is a symmetric positive definite  $2 \times 2$  matrix, of coefficients in  $L^\infty(\Omega)$ . For the sake of simplicity, we take in what follows  $K = k\mathbb{I}_2$  with  $k \in L^\infty(\Omega)$  and  $k(x) \geq k_0 > 0$  a.e in  $\Omega$ . For any  $\chi \in H^{1/2}(\Gamma_D)$ , let

$$V^\chi = \{v \in H^1(\Omega) : v = \chi \text{ on } \Gamma_D\}.$$

The primal weak formulation associated to the previous boundary problem reads:

$$u \in V^{g_D}, \quad a(u, v) = (f, v)_\Omega + (g_N, v)_{\Gamma_N} \quad \forall v \in V^0,$$

where  $a(u, v) = (K\nabla u, \nabla v)_\Omega$ . Thanks to the Lax-Milgram lemma, there exists a unique solution to this problem.

In the following, we introduce some notation. We denote by  $\mathcal{T}_h$  a regular mesh consisting of triangles, such that the domain's boundary  $\partial\Omega$  is covered by the Dirichlet and Neumann sides,  $\mathcal{F}_h^D$  and  $\mathcal{F}_h^N$ , respectively. We denote by  $\mathcal{F}_h^{int}$  the set of interior sides and we put  $\mathcal{F}_h = \mathcal{F}_h^{int} \cup \mathcal{F}_h^D$ . We denote by  $\mathcal{N}_h^{int}$  and  $\mathcal{N}_h^\partial$  the set of nodes which

are interior to the domain  $\Omega$  or situated on  $\partial\Omega$ , respectively. We assume, for the sake of simplicity, that a cell  $T \in \mathcal{T}_h$  cannot have all three vertices on  $\Gamma_N$ .

For a interior side  $F$ ,  $n_F$  is a fixed, arbitrary, unit vector normal to  $F$ , oriented from  $T^-$  towards  $T^+$ , where  $T^-, T^+$  are the two triangles sharing the side  $F$ . If the side  $F$  lies on  $\partial\Omega$ , we set  $n_F = n$ .

We define the following spaces of piecewise polynomial functions of degree  $l \in \mathbb{N}$  on the cells and the sides, respectively :

$$\begin{aligned}\mathcal{D}_h^l &= \{v_h \in L^2(\mathcal{T}_h) : v_h|_T \in P^l(T) \quad \forall T \in \mathcal{T}_h\}, \\ \mathcal{C}_h^l &= \mathcal{D}_h^l \cap \mathcal{C}^0(\bar{\Omega}), \\ \mathcal{M}_h^l &= \{\mu_h \in L^2(\mathcal{F}_h^{int}) : \mu_h|_F \in P^l(F) \quad \forall F \in \mathcal{F}_h^{int}\}.\end{aligned}$$

For the sake of simplicity, we assume that  $K$  is piecewise constant. Let  $v \in \mathcal{D}_h^l$ . For a given  $F \in \mathcal{F}_h^{int}$  and  $x \in F$ , we define as usually:

$$v_F^+(x) = \lim_{\varepsilon \rightarrow 0^+} v(x + \varepsilon n_F), \quad v_F^-(x) = \lim_{\varepsilon \rightarrow 0^+} v(x - \varepsilon n_F),$$

as well as the jump and weighted means at  $x \in F$ , by

$$[v]_F = v_F^- - v_F^+, \quad \{v\}_F = \omega^+ v_F^+ + \omega^- v_F^-, \quad \{v\}_F^* = \omega^- v_F^+ + \omega^+ v_F^-,$$

where (cf. for instance [25]):

$$\omega^+ = \frac{k^-}{k^+ + k^-}, \quad \omega^- = \frac{k^+}{k^+ + k^-}, \quad k^\pm = k|_{T^\pm}. \quad (2.2)$$

We also introduce the stabilisation parameter  $k_F = \frac{k^+ k^-}{k^+ + k^-}$ . For a boundary side  $F$ , we set  $[v]_F = \{v\}_F = v_F^-$  and  $k_F = k^-$ . It is useful to note that, for any  $F \in \mathcal{F}_h$ ,

$$0 \leq \omega^\pm \leq 1, \quad \omega^+ + \omega^- = 1, \quad k_F = k^\pm \omega^\pm \leq k^\pm. \quad (2.3)$$

In the sequel, we will omit the index  $F$  in the jump and the means whenever possible. We will also use the following notation for the piecewise integration:

$$\int_{\mathcal{T}_h} = \sum_{T \in \mathcal{T}_h} \int_T, \quad \int_{\mathcal{F}_h} = \sum_{F \in \mathcal{F}_h} \int_F.$$

We recall the well-known trace inequality, for  $T \in \mathcal{T}_h$  and  $F \subset \partial T$ :

$$|F|^{-1/2} \|v\|_{0,F} \lesssim \frac{1}{d_T} \|v\|_{0,T} + |v|_{1,T}, \quad \forall v \in H^1(T). \quad (2.4)$$

**3. Discrete problem and equivalent mixed formulation.** We consider successively conforming and nonconforming finite element discretizations.

**3.1. Conforming approximation.** We first discretize problem (2.1) by means of conforming finite elements. We use Nitsche's method to treat the Dirichlet boundary condition. For the simplicity of presentation, we consider in what follows the piecewise linear case ( $l = 1$ ) but the theory holds for arbitrary  $l \in \mathbb{N}^*$ , cf. [10] for the

Poisson equation. Let the bilinear and linear forms, for any  $u_h, v_h \in \mathcal{C}_h^1$ :

$$\begin{aligned} a_h(u_h, v_h) &= \int_{\mathcal{T}_h} K \nabla u_h \cdot \nabla v_h \, dx - \int_{\mathcal{F}_h^D} (K \nabla u_h \cdot n v_h + K \nabla v_h \cdot n u_h) \, ds \\ &\quad + \gamma \int_{\mathcal{F}_h^D} \frac{k_F}{|F|} v_h u_h \, ds, \\ l_h(v_h) &= \int_{\mathcal{T}_h} f v_h \, dx + \int_{\Gamma_N} g_N v_h \, ds - \int_{\mathcal{F}_h^D} K \nabla v_h \cdot n g_D \, ds + \gamma \int_{\mathcal{F}_h^D} \frac{k_F}{|F|} v_h g_D \, ds, \end{aligned}$$

where  $\gamma > 0$  is a stabilisation parameter independent of  $h$  and  $K$ .

We consider the discrete problem:

$$u_h \in \mathcal{C}_h^1, \quad a_h(u_h, v_h) = l_h(v_h) \quad \forall v_h \in \mathcal{C}_h^1. \quad (3.1)$$

We use the following semi-norm and norm on  $H^1(\Omega)$ :

$$|v|_{1,K} = \|K^{1/2} \nabla v\|_{0,\Omega}, \quad |||v||| = \left( |v|_{1,K}^2 + \int_{\mathcal{F}_h^D} \frac{k_F}{|F|} v^2 \, ds \right)^{1/2}.$$

It is well-known that for  $\gamma$  large enough,  $a_h(\cdot, \cdot)$  is  $|||\cdot|||$ -coercive on  $\mathcal{C}_h^1 \times \mathcal{C}_h^1$ , uniformly with respect to both  $h$  and  $K$ . The existence and uniqueness of the solution of (3.1) follows from the Lax-Milgram lemma.

Following [10], we introduce a hybrid mixed formulation with an additional unknown  $\theta_h$  defined on the interior sides of the mesh. The continuity of  $u_h$  across the interior sides is dualized by means of a multiplier. Note that in [10], the Dirichlet boundary condition was imposed strongly, leading to a multiplier defined on both the interior and the Dirichlet sides.

The multiplier  $\theta_h$  is then used in order to recover the numerical conservative flux. It is important to note that we do not solve the global mixed formulation, but we compute  $\theta_h$  locally. For this purpose, let us first introduce the space

$$\mathcal{M}_h = \left\{ \mu_h \in \mathcal{M}_h^1; \sum_{F \in \mathcal{F}_N} \mathfrak{s}_{N,F} |F| \mu_h|_F(N) = 0 \quad \forall N \in \mathcal{N}_h^{int} \right\},$$

where  $\mathcal{F}_N$  is the set of sides sharing the node  $N \in \mathcal{N}_h^{int}$  and  $\mathfrak{s}_{N,F}$  is the sign function, which is equal to 1 or  $-1$  depending upon the orientation of  $n_F$  with respect to the clockwise rotation sense around  $N$ . The auxiliary mixed formulation is given by: find  $(\tilde{u}_h, \theta_h) \in \mathcal{D}_h^1 \times \mathcal{M}_h$  such that

$$\begin{aligned} \tilde{a}_h(\tilde{u}_h, v_h) + b_h(\theta_h, v_h) &= l_h(v_h) \quad \forall v_h \in \mathcal{D}_h^1, \\ b_h(\mu_h, \tilde{u}_h) &= 0 \quad \forall \mu_h \in \mathcal{M}_h, \end{aligned} \quad (3.2)$$

where

$$\begin{aligned} \tilde{a}_h(\tilde{u}_h, v_h) &= a_h(\tilde{u}_h, v_h) - \int_{\mathcal{F}_h^{int}} \{K \nabla \tilde{u}_h \cdot n_F\} [v_h] \, ds - \int_{\mathcal{F}_h^{int}} \{K \nabla v_h \cdot n_F\} [\tilde{u}_h] \, ds, \\ b_h(\mu_h, v_h) &= \sum_{F \in \mathcal{F}_h^{int}} \frac{k_F |F|}{2} \sum_{N \in \mathcal{N}_F} \mu_h|_F(N) [v_h]_F(N), \end{aligned}$$

with  $\mathcal{N}_F$  the set of vertices of  $F$ . Note that  $b_h(\mu_h, v_h)$  is the approximation of  $\int_{\mathcal{F}_h^{int}} k_F \mu_h [v_h] ds$  by the trapeze formula (or, for an arbitrary degree  $l$ , by the Gauss-Lobatto integration formula with  $l+1$  points).

We first show that the solution  $\tilde{u}_h$  of the mixed formulation (3.2) coincides with the solution  $u_h$  of the original discrete problem (3.1).

LEMMA 3.1. *The discrete kernel of  $b_h(\cdot)$  coincides with the space  $\mathcal{C}_h^1$ , i.e.,*

$$\text{Ker } b_h = \{v_h \in \mathcal{D}_h^1; b_h(\mu_h, v_h) = 0, \forall \mu_h \in \mathcal{M}_h\} = \mathcal{C}_h^1.$$

*Proof.* Obviously,  $\mathcal{C}_h^1 \subset \text{Ker } b_h$ . Now let any  $v_h \in \text{Ker } b_h$  and consider the function  $\mu_h$  defined by  $\mu_h|_F = |F|^{-1}[v_h]_F$  for any  $F \in \mathcal{F}_h^{int}$ . Clearly,  $\mu_h$  belongs to  $\mathcal{M}_h$  because

$$\forall N \in \mathcal{N}_h^{int}, \quad \sum_{F \in \mathcal{F}_N} \mathfrak{s}_{N,F} |F| \mu_h|_F(N) = \sum_{F \in \mathcal{F}_N} \mathfrak{s}_{N,F} [v_h]_F = 0.$$

From  $b_h(\mu_h, v_h) = 0$  we get  $[v_h]_F = 0$  for any  $F \in \mathcal{F}_h^{int}$ , which yields  $v_h \in \mathcal{C}_h^1$ .  $\square$

Thus,  $\tilde{u}_h$  satisfies (3.1) and the uniqueness of its solution yields  $\tilde{u}_h = u_h$ .

We next establish the well-posedness of the mixed formulation. For this purpose, we introduce the following discrete norms:

$$\begin{aligned} \|v_h\|_h &= \left( \int_{\mathcal{T}_h} K \nabla v_h \cdot \nabla v_h dx + \int_{\mathcal{F}_h} |F|^{-1} k_F [v_h]^2 ds \right)^{1/2}, \quad v_h \in \mathcal{D}_h^1, \\ \|\mu_h\|_{\mathcal{M}_h} &= \left( \int_{\mathcal{F}_h^{int}} |F| k_F \mu_h^2 ds \right)^{1/2}, \quad \mu_h \in \mathcal{M}_h^1 \end{aligned}$$

and we recall the following inequality (see for instance [7]), which holds uniformly with respect to  $h$  and  $K$ :

$$\forall v_h \in \mathcal{D}_h^1, \quad \int_{\mathcal{F}_h} |F| k_F^{-1} \{K \nabla v_h \cdot n_F\}^2 ds \lesssim \int_{\mathcal{T}_h} K \nabla v_h \cdot \nabla v_h dx. \quad (3.3)$$

Thanks to (3.3) and to the Cauchy-Schwarz inequality, one immediately obtains the uniform continuity of the bilinear forms: for any  $\mu_h \in \mathcal{M}_h$  and  $u_h, v_h \in \mathcal{D}_h^1$ ,

$$\tilde{a}_h(u_h, v_h) \lesssim \|u_h\|_h \|v_h\|_h, \quad b_h(\mu_h, v_h) \lesssim \|v_h\|_h \|\mu_h\|_{\mathcal{M}_h}.$$

Lemma 3.1 yields the uniform  $\|\cdot\|_h$ -coercivity of  $\tilde{a}_h(\cdot, \cdot)$  on  $\text{Ker } b_h$  for  $\gamma$  large enough. In order to apply the Babuska-Brezzi theorem to the mixed problem (3.2), we establish the inf-sup condition for  $b_h(\cdot, \cdot)$ . The proof is similar to [10] for the Poisson problem and is given in the Appendix. The difference is that we track the robust dependence of the inf-sup constant on the diffusion coefficient  $K$ .

DEFINITION 3.2.  *$K$  is quasi-monotone on  $\omega_N$  if there exists a clockwise or counter-clockwise complete path along which  $K$  is monotone.  $K$  is said to be quasi-monotone on  $\mathcal{T}_h$  if it is quasi-monotone for every  $\omega_N, N \in \mathcal{N}_h$ .*

LEMMA 3.3. *Assume  $K$  is quasi-monotone. There exists a constant  $\beta > 0$  independent of  $h$ ,  $\gamma$  and  $K$  such that*

$$\inf_{\mu_h \in \mathcal{M}_h} \sup_{v_h \in \mathcal{D}_h^1} \frac{b_h(\mu_h, v_h)}{\|\mu_h\|_{\mathcal{M}_h} \|v_h\|_h} \geq \beta.$$

The proof of the lemma is provided in the appendix.

**3.2. Nonconforming approximation.** We now consider a nonconforming approximation based on the finite element space of arbitrary polynomial degree  $k \in \mathbb{N}^*$  introduced in [22]. We begin by recalling its definition. Let  $T \in \mathcal{T}_h$  and let

$$\Sigma_{k+1}(T) = \text{span}\{b_T \varphi_{T,1}^{k-2-i} \varphi_{T,2}^i; i = 0, \dots, k-2\} \subset P^{k+1}(T), \quad (3.4)$$

where  $\{\varphi_{T,i}; 1 \leq i \leq 3\}$  denote the barycentric coordinates of the triangle  $T$  and

$$b_T = (\varphi_{T,1} - \varphi_{T,2})(\varphi_{T,2} - \varphi_{T,3})(\varphi_{T,3} - \varphi_{T,1}).$$

Consider the following enriched space

$$V_k(T) = P^k(T) \oplus \Sigma_{k+1}(T)$$

and define the nodal basis functions as follows:

$$\begin{aligned} N_{F,i}^T(v) &= \frac{1}{|F|} \int_F v L_i ds, \quad 0 \leq i \leq k-1, \quad F \in \mathcal{F}_h \cap \partial T \\ N_j^T(v) &= \frac{1}{|T|} \int_T v M_j^T dx, \quad 1 \leq j \leq \frac{k(k-1)}{2}, \end{aligned} \quad (3.5)$$

where  $\{M_j^T\}$  is an arbitrary but fixed basis of  $P^{k-2}(T)$  and  $L_j$  is the  $j$ -th order Legendre polynomial. Let  $\phi_{F,i}$ , for  $0 \leq i \leq k-1$  and  $\phi_j$ , for  $1 \leq j \leq \frac{k(k-1)}{2}$  be the corresponding nodal basis functions.

The discontinuous and nonconforming spaces  $\mathcal{DG}_h^k$  and  $\mathcal{NC}_h^k$  are defined as follows:

$$\begin{aligned} \mathcal{DG}_h^k &= \{v_h \in L^2(\Omega); v_h|_T \in V_k(T), \forall T \in \mathcal{T}_h\}, \\ \mathcal{NC}_h^k &= \left\{v_h \in \mathcal{DG}_h^k; \int_F [v_h] p ds = 0, \forall F \in \mathcal{F}_h^{int}, \forall p \in P^{k-1}(F)\right\}. \end{aligned}$$

We consider the following discrete version of (2.1): find  $u_h^* \in \mathcal{NC}_h^k$  such that

$$a_h(u_h^*, v_h) = l_h(v_h) \quad \forall v_h \in \mathcal{NC}_h^k, \quad (3.6)$$

which is well-posed. We introduce the auxiliary mixed formulation: find  $(\tilde{u}_h^*, \theta_h^*) \in \mathcal{DG}_h^k \times \mathcal{M}_h^{k-1}$  such that

$$\begin{aligned} \tilde{a}_h^*(\tilde{u}_h^*, v_h) + b_h^*(\theta_h^*, v_h) &= l_h(v_h) \quad \forall v_h \in \mathcal{DG}_h^k, \\ b_h^*(\mu_h, \tilde{u}_h^*) &= 0 \quad \forall \mu_h \in \mathcal{M}_h^{k-1}, \end{aligned} \quad (3.7)$$

where

$$\begin{aligned} \tilde{a}_h^*(\tilde{u}_h^*, v_h) &= a_h(\tilde{u}_h^*, v_h) - \int_{\mathcal{F}_h^{int}} \left( \pi_F^{k-1} \{K \nabla \tilde{u}_h^* \cdot n_F\} [v_h] + \pi_F^{k-1} \{K \nabla v_h \cdot n_F\} [\tilde{u}_h^*] \right) ds, \\ b_h^*(\mu_h, v_h) &= \int_{\mathcal{F}_h^{int}} \mu_h [v_h] ds \end{aligned}$$

and where  $\pi_F^{k-1}$  stands for the  $L^2(F)$ -orthogonal projection on  $P^{k-1}(F)$ .

Note that one is now able to get rid of the coefficient  $k_F$  in the bilinear form  $b_h^*(\cdot, \cdot)$  because there is no linear constraint in the space  $\mathcal{M}_h^{k-1}$ . Since the multipliers are  $P^{k-1}$ -functions on each interior side, we immediately obtain that

$$\text{Ker } b_h^* = \left\{v_h \in \mathcal{DG}_h^k : b_h^*(\mu_h, v_h) = 0, \forall \mu_h \in \mathcal{M}_h^{k-1}\right\} = \mathcal{NC}_h^k.$$



179 So the primal and mixed formulations (3.6) and (3.7) are equivalent, i.e.  $\tilde{u}_h^* = u_h^*$ .

We are next interested in the well-posedness of the mixed formulation (3.7). The continuity of  $\tilde{a}_h^*(\cdot, \cdot)$  is similar to the conforming case. The space  $\mathcal{M}_h^{k-1}$  is now endowed with the norm:

$$\|\mu_h\|_{\mathcal{N}C_h}^2 = \int_{\mathcal{F}_h^{int}} k_F^{-1} |F| \mu_h^2 ds, \quad \forall \mu_h \in \mathcal{M}_h^{k-1},$$

180 which immediately yields  $b_h^*(\mu_h, v_h) \leq \|\mu_h\|_{\mathcal{N}C_h} \|v_h\|_h$ . So we only have to establish  
 181 the inf-sup condition for  $b_h^*(\cdot, \cdot)$ .

LEMMA 3.4. *There exists a constant  $\beta^*$  independent of  $h$ ,  $\gamma$  and  $K$  such that*

$$\inf_{\mu_h \in \mathcal{M}_h^{k-1}} \sup_{v_h \in \mathcal{DG}_h^k} \frac{b_h^*(\mu_h, v_h)}{\|\mu_h\|_{\mathcal{N}C_h} \|v_h\|_h} \geq \beta^*.$$

182 *Proof.* We construct a Fortin operator, which associates to any  $\mu_h \in \mathcal{M}_h^{k-1}$  a  
 183 unique function  $v_h \in \mathcal{DG}_h^k$  satisfying

$$b_h^*(\mu_h, v_h) \gtrsim \|\mu_h\|_{\mathcal{N}C_h}^2, \quad \|v_h\|_h \lesssim \|\mu_h\|_{\mathcal{N}C_h}. \quad (3.8)$$

184 For any  $F \in \mathcal{F}_h^{int}$ , let  $\Delta_F = T^+ \cup T^-$  the patch consisting of the triangles sharing  
 185 the side  $F$ . The construction of  $v_h$  is achieved patch-wise:  $v_h = \sum_{F \in \mathcal{F}_h^{int}} v_F$  with  $v_F$

186 defined on  $\Delta_F$ . Since  $\mu_h|_F \in P^{k-1}$ , we can write it in the Legendre basis of  $P^{k-1}$ :

$$\exists! (\alpha_0, \dots, \alpha_{k-1}) \in \mathbb{R}^k, \quad \mu_h|_F = \sum_{j=0}^{k-1} \alpha_j L_j.$$

187 Then we define  $v_F$  as follows:

$$(v_F)|_{T^+} = \frac{|F|}{k^+} \sum_{i=0}^{k-1} \alpha_i \phi_{F,i}, \quad (v_F)|_{T^-} = \frac{|F|}{k^-} \sum_{i=0}^{k-1} \alpha_i \phi_{F,i}. \quad (3.9)$$

This choice directly yields that  $v_F \in \mathcal{DG}_h^k$  and  $[v_h]_F = k_F^{-1} |F| \sum_{i=0}^{k-1} \alpha_i \phi_{F,i}$ . Hence,

$$\int_F \mu_h [v_h] ds = k_F^{-1} |F| \sum_{i,j=0}^{k-1} \alpha_i \alpha_j \int_F L_j \phi_{F,i} ds = k_F^{-1} |F|^2 \sum_{j=0}^{k-1} \alpha_j^2,$$

188 thanks to the definition of the nodal basis functions  $\phi_{F,i}$ . Noting that

$$\int_F \mu_h^2 ds = \int_F \left( \sum_{j=0}^{k-1} \alpha_j L_j \right)^2 ds = \sum_{j=0}^{k-1} \alpha_j^2 \|L_j\|_{0,F}^2 \approx |F| \sum_{j=0}^{k-1} \alpha_j^2, \quad (3.10)$$

189 we deduce that

$$b_h^*(\mu_h, v_h) = \sum_{F \in \mathcal{F}_h^{int}} \int_F \mu_h [v_h] ds \approx \|\mu_h\|_{\mathcal{N}C_h}^2. \quad (3.11)$$

We still have to establish the second bound of (3.8). For any  $F \in \mathcal{F}_h^{int}$ , we have that:

$$\frac{k_F}{|F|} \|[v_h]\|_{0,F}^2 \leq \frac{|F|}{k_F} \left( \sum_{i=0}^{k-1} \alpha_i^2 \right) \left( \sum_{i=0}^{k-1} \|\phi_{F,i}\|_{0,F}^2 \right) \lesssim \frac{|F|^2}{k_F} \sum_{i=0}^{k-1} \alpha_i^2 \lesssim \frac{|F|}{k_F} \|\mu_h\|_{0,F}^2.$$

190 A similar bound is obtained on any Dirichlet side, which finally leads to

$$\int_{\mathcal{F}_h} k_F |F|^{-1} [v_h]^2 \lesssim \|\mu_h\|_{\mathcal{NC}_h}^2. \quad (3.12)$$

We next have, using first  $(v_h)|_T = \sum_{F \in \partial T \cap \mathcal{F}_h^{int}} v_F$  and then (3.9), that

$$\begin{aligned} \int_{\mathcal{T}_h} K \nabla v_h \cdot \nabla v_h dx &= \sum_{T \in \mathcal{T}_h} k_T |v_h|_{1,T}^2 \lesssim \sum_{F \in \mathcal{F}_h^{int}} \sum_{T \in \Delta_F} k_T |v_F|_{1,T}^2 \\ &\leq \sum_{F \in \mathcal{F}_h^{int}} \sum_{T \in \Delta_F} \frac{|F|^2}{k_T} \left( \sum_{i=0}^{k-1} |\alpha_i| |\phi_{F,i}|_{1,T} \right)^2. \end{aligned}$$

191 Since  $|\phi_{F,i}|_{1,T} \leq C$  and  $k_F \leq k^\pm$ , it follows thanks to (3.10) that

$$\int_{\mathcal{T}_h} K \nabla v_h \cdot \nabla v_h dx \lesssim \sum_{F \in \mathcal{F}_h^{int}} \frac{|F|^2}{k_F} \left( \sum_{i=0}^{k-1} \alpha_i^2 \right) \lesssim \sum_{F \in \mathcal{F}_h^{int}} \frac{|F|}{k_F} \|\mu_h\|_{0,F}^2 = \|\mu_h\|_{\mathcal{NC}_h}^2. \quad (3.13)$$

192 We can now conclude thanks to (3.11), (3.12) and (3.13).  $\square$

193 **4. Local computation of the multiplier.** Again, we discuss successively the  
194 conforming and nonconforming cases.

**4.1. Conforming approximation.** Let the functional

$$r_h(\cdot) = l_h(\cdot) - \tilde{a}_h(u_h, \cdot).$$

195 Thanks to the mixed formulation, we have  $r_h(v_h) = 0$  for any  $v_h \in \mathcal{C}_h^1$ . Moreover,  $\theta_h$   
196 is uniquely defined in  $\mathcal{M}_h$  by

$$b_h(\theta_h, v_h) = r_h(v_h) \quad \forall v_h \in \mathcal{D}_h^1. \quad (4.1)$$

It is useful to introduce, for any interior side  $F$  of vertices  $N, M$ , the bilinear form

$$b_F(\theta, \varphi) = \frac{|F|k_F}{2} (\theta(N)\varphi(N) + \theta(M)\varphi(M)).$$

197 Let  $N \in \mathcal{N}_h$ . We define  $\theta_N \in \mathcal{M}_h$  on  $\mathcal{F}_N \cap \mathcal{F}_h^{int}$  such that, for any  $T \in \omega_N$ ,

$$b_h(\theta_N, \varphi_N \chi_T) = r_h(\varphi_N \chi_T), \quad (4.2)$$

$$b_h(\theta_N, \varphi_M \chi_T) = 0, \quad \forall M \in \mathcal{N}_T \setminus \{N\} \quad (4.3)$$

198 with  $\varphi_N, \varphi_M$  the  $P^1$ -nodal basis functions and  $\chi_T$  the characteristic function on  $T$ .  
199 We impose moreover  $\theta_N = 0$  on  $\mathcal{F}_h^{int} \setminus \mathcal{F}_N$ .

200 The next result shows that the multiplier  $\theta_h$  can be computed locally. We refer  
201 to [10] for the proof, which is based on (4.1).

LEMMA 4.1. Let  $\theta_h$  and  $\theta_N$  be the solutions of (3.2) and (4.2)-(4.3), respectively. Then

$$\theta_h = \sum_{N \in \mathcal{N}_h} \theta_N. \quad (4.4)$$

In what follows, we study the linear system (4.2)-(4.3). Note that (4.3) immediately yields  $(\theta_N)|_F(M) = 0$  for all  $F \in \mathcal{F}_N$ , where  $M$  denotes the other vertex of  $F$ ; thus,  $\theta_N$  obviously satisfies the constraint of the space  $\mathcal{M}_h$  at all the interior nodes  $M$  different from  $N$ . Therefore, we only need to consider (4.2). As in [10], it can be shown that it has a unique solution in  $\mathcal{M}_h$ .

We next focus on the bound of  $\theta_N$ . For this purpose, let  $n_N$  denote the number of elements in  $\omega_N$ , ordered clockwise from  $T_1$  to  $T_{n_N}$ , with  $T_1$  the element such that  $k|_{T_1} = \max_{T \subset \omega_N} k_T$  if  $N$  is a interior node and  $T_1$  containing a boundary side otherwise. We set  $F_i = \partial T_i \cap \partial T_{i+1}$ , with  $T_{n_N+1} = T_1$  and  $i \in \{1, \dots, n_N\}$  if  $N \in \mathcal{N}_h^{int}$ , and  $i \in \{1, \dots, n_N-1\}$  if  $N \in \mathcal{N}_h^\partial$ . We recall that the sign coefficient  $\mathfrak{s}_i := \mathfrak{s}_{N, F_i}$  equals  $\pm 1$  if  $T_i = T^\mp$  with respect to  $F_i$ . Let also  $x_i := \mathfrak{s}_i k_{F_i} |F_i| (\theta_N)|_{F_i}(N)$  and  $b_i := 2r_h(\varphi_N \chi_{T_i})$ .

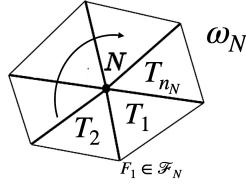


Fig. 4.1: Patch  $\omega_N$  around a node  $N$

We now introduce the following constant, for any  $N \in \mathcal{N}_h$ :

$$C_N := \max_{1 \leq j \leq i \leq n_N} \frac{\sqrt{k_i}}{\sqrt{k_j}} \quad \text{where} \quad k_i = k|_{T_i}. \quad (4.5)$$

Clearly,  $C_N = 1$  if the coefficient  $K$  is quasi-monotone.

For  $N \in \mathcal{N}_h^{int}$ , the local system (4.2) together with the condition  $\theta_N \in \mathcal{M}_h$  translates into the following matrix equation:

$$x_i - x_{i-1} = 2b_i \quad (1 \leq i \leq n_N), \quad \sum_{i=1}^{n_N} k_{F_i}^{-1} x_i = 0, \quad (4.6)$$

where  $x_0 = x_{n_N}$ . A simple calculation yields that the solution of (4.6) is given by:

$$x_i = \sum_{j=1}^i \frac{\bar{\Lambda}_j}{\Lambda_1} b_j - \sum_{j=i+1}^{n_N} \frac{\Lambda_j}{\Lambda_1} b_j, \quad 1 \leq i < n_N, \quad x_{n_N} = \sum_{j=1}^{n_N} \frac{\bar{\Lambda}_j}{\Lambda_1} b_j, \quad (4.7)$$

where  $\Lambda_j = \sum_{l=j}^{n_N} k_{F_l}^{-1}$ ,  $\bar{\Lambda}_j = \Lambda_1 - \Lambda_j$  for  $1 \leq j \leq n_N$ .

For  $N \in \mathcal{N}_h^\partial$ , since  $\theta_N$  is defined only on the interior sides and no constraint at the node  $N$  is imposed in the space  $\mathcal{M}_h$ , system (4.2) translates into:

$$x_i - x_{i-1} = 2b_i \quad (1 \leq i \leq n_N - 1) \quad (4.8)$$

where  $x_0 = 0$  here. Its solution is given by  $x_i = 2 \sum_{j=1}^i b_j = -2 \sum_{j=i+1}^{n_N} b_j$  for  $1 \leq i \leq n_N - 1$ .

LEMMA 4.2. For any  $N \in \mathcal{N}_h$ , we have that:

$$k_{F_i}^{-1/2} |x_i| \lesssim \mathcal{C}_N \sum_{j=1}^{n_N} k_j^{-1/2} |b_j|, \quad 1 \leq i \leq n_N. \quad (4.9)$$

*Proof.* We detail the proof for  $N \in \mathcal{N}_h^{int}$ , the case of a boundary node being similar. By using that  $0 < \frac{\Lambda_j}{\Lambda_1} \leq 1$  for  $2 \leq j \leq n_N$ , we first get from (4.7) that

$$|x_1| \leq \sum_{j=2}^{n_N} |b_j|, \text{ which gives that}$$

$$k_{F_1}^{-1/2} |x_1| \leq \sum_{j=2}^{n_N} (k_{F_1}^{-1/2} k_j^{1/2}) k_j^{-1/2} |b_j|.$$

Since  $k_{F_1}^{-1} = k_1^{-1} + k_2^{-1}$ , we clearly have  $k_{F_1}^{-1/2} k_j^{1/2} \leq 2\mathcal{C}_N$ , which yields (4.9) for  $i = 1$ .

Using now the expression of  $x_i$  for  $i \geq 2$  from (4.7) we obtain:

$$k_{F_i}^{-1/2} |x_i| \leq \sum_{j=2}^i \frac{\bar{\Lambda}_j}{\Lambda_1} k_{F_i}^{-1/2} |b_j| + \sum_{j=i+1}^{n_N} \frac{\Lambda_j}{\Lambda_1} k_{F_i}^{-1/2} |b_j|, \quad 2 \leq i \leq n_N - 1 \quad (4.10)$$

$$k_{F_{n_N}}^{-1/2} |x_{n_N}| \leq \sum_{j=2}^{n_N} \frac{\bar{\Lambda}_j}{\Lambda_1} k_{F_i}^{-1/2} |b_j|. \quad (4.11)$$

The second sum in (4.10) is bounded similarly to the case of  $x_1$ . We use  $0 < \frac{\Lambda_j}{\Lambda_1} \leq 1$

and  $k_{F_i}^{-1} = k_i^{-1} + k_{i+1}^{-1}$  and we thus get:

$$\sum_{j=i+1}^{n_N} \frac{\Lambda_j}{\Lambda_1} k_{F_i}^{-1/2} |b_j| \leq \sum_{j=i+1}^{n_N} (k_{F_i}^{-1/2} k_j^{1/2}) k_j^{-1/2} |b_j| \leq 2\mathcal{C}_N \sum_{j=i+1}^{n_N} k_j^{-1/2} |b_j|. \quad (4.12)$$

As regards the first sum in (4.10) and in (4.11), we first use that  $\Lambda_1 \geq k_{F_i}^{-1} + k_{F_l}^{-1}$  for any indices  $i, l$  in order to obtain, for any index  $j$  such that  $2 \leq j \leq i$ ,

$$\frac{\bar{\Lambda}_j}{\Lambda_1} k_{F_i}^{-1/2} |b_j| = \left( \sum_{l=1}^{j-1} k_{F_l}^{-1} \right) \frac{k_{F_i}^{-1/2}}{\Lambda_1} |b_j| = \sum_{l=1}^{j-1} \frac{k_{F_l}^{-1} k_{F_i}^{-1/2}}{\Lambda_1} |b_j| \leq \sum_{l=1}^{j-1} k_{F_l}^{-1/2} \frac{k_{F_l}^{-1/2} k_{F_i}^{-1/2}}{k_{F_l}^{-1} + k_{F_i}^{-1}} |b_j|.$$

Thanks to the mean inequality, we further get

$$\frac{\bar{\Lambda}_j}{\Lambda_1} k_{F_i}^{-1/2} |b_j| \leq \frac{1}{2} \sum_{l=1}^{j-1} k_{F_l}^{-1/2} |b_j| = \frac{1}{2} \left( \sum_{l=1}^{j-1} k_{F_l}^{-1/2} k_j^{1/2} \right) k_j^{-1/2} |b_j|.$$

Since  $l+1 \leq j$ , the same argument as above, namely  $k_{F_l}^{-1/2} k_j^{1/2} \leq 2\mathcal{C}_N$ , yields that

$$\frac{\bar{\Lambda}_j}{\Lambda_1} k_{F_i}^{-1/2} |b_j| \leq (j-1) \mathcal{C}_N k_j^{-1/2} |b_j|, \quad 2 \leq j \leq i.$$

Since  $n_N$  is uniformly bounded, we next get:

$$\sum_{j=2}^i \frac{\bar{\Lambda}_j}{\Lambda_1} k_{F_i}^{-1/2} |b_j| \lesssim \mathcal{C}_N \sum_{j=2}^i k_j^{-1/2} |b_j|. \quad (4.13)$$

Finally, using (4.12) and (4.13) in (4.10) yields the result for  $2 \leq i \leq n_N$ .  $\square$

We can now deduce the next bound for  $\theta_N$ , with respect to the local norm

$$\|\mu_h\|_{\mathcal{F}_N}^2 := \sum_{F \in \mathcal{F}_N \cap \mathcal{F}_h^{int}} \int_F |F| k_F^{-1} \mu_h^2 ds, \quad \mu_h \in \mathcal{M}_h.$$

LEMMA 4.3.

For any  $N \in \mathcal{N}_h$ , one has that:

$$\|\theta_N\|_{\mathcal{F}_N} \lesssim \mathcal{C}_N \sum_{T \in \omega_N} k_T^{-1/2} |r_h(\varphi_N \chi_T)|. \quad (4.14)$$

*Proof.* The definition of  $\theta_N$  yields that  $\|\theta_N\|_{\mathcal{F}_N}^2 = \frac{1}{3} \sum_{i=1}^{m_N} k_{F_i}^{-1} x_i^2$ , with  $m_N := n_N$  if  $N \in \mathcal{N}_h^{int}$  and  $m_N := n_N - 1$  if  $N \in \mathcal{N}_h^\partial$ . The result follows from Lemma 4.2.  $\square$

We are now able to prove the main result of this section. For  $l \in \mathbb{N}$ , we denote by  $\pi_\omega^l$  the  $L^2(\omega)$ -orthogonal projection on  $P^l(\omega)$ .

THEOREM 4.4. For any  $N \in \mathcal{N}_h$ , the local multiplier satisfies the bound:

$$\begin{aligned} \|\theta_N\|_{\mathcal{F}_N} &\lesssim \mathcal{C}_N \sum_{T \in \omega_N} \left( \frac{h_T}{k_T^{1/2}} \|\pi_T^1 f\|_{0,T} + \sum_{F \in \partial T \cap \mathcal{F}_h^{int}} \frac{\bar{\omega}_{F,T} h_F^{1/2}}{k_T^{1/2}} \| [K \nabla u_h \cdot n_F] \|_{0,F \cap \mathcal{F}_N} \right. \\ &\quad \left. + \sum_{F \in \partial T \cap \Gamma_D} \frac{k_F^{1/2}}{h_F^{1/2}} \| u_h - \pi_F^1 g_D \|_{0,F \cap \mathcal{F}_N} + \sum_{F \in \partial T \cap \Gamma_N} \frac{h_F^{1/2}}{k_F^{1/2}} \| K \nabla u_h \cdot n - \pi_F^1 g_N \|_{0,F \cap \mathcal{F}_N} \right) \end{aligned}$$

where  $\bar{\omega}_{F,T} = \omega_F^\pm$  if  $T = T^\mp$  with respect to  $n_F$ .

*Proof.* Let any  $T \in \omega_N$ . Using that  $[u_h]_F = 0$  for any  $F \in \mathcal{F}_h^{int}$ , we have that:

$$\begin{aligned} r_h(\varphi_N \chi_T) &= l_h(\varphi_N \chi_T) - \tilde{a}_h(u_h, \varphi_N \chi_T) \\ &= \int_T f \varphi_N dx + \int_{\partial T \cap \Gamma_N} g_N \varphi_N ds - \int_{\partial T \cap \Gamma_D} K \nabla \varphi_N \cdot n (g_D - u_h) ds \\ &\quad + \int_{\partial T \cap \Gamma_D} \frac{\gamma k_F}{|F|} \varphi_N (g_D - u_h) ds - \int_T K \nabla u_h \cdot \nabla \varphi_N dx \\ &\quad + \int_{\partial T \cap \Gamma_D} K \nabla u_h \cdot n \varphi_N ds + \int_{\partial T \cap \mathcal{F}_h^{int}} \{K \nabla u_h \cdot n_F\} [\varphi_N \chi_T] ds. \end{aligned}$$

Thanks to integration by parts and to the well-known formula  $[ab] = \{a\}[b] + [a]\{b\}^*$ , we obtain, since  $K \nabla u_h$  is constant on  $T$ , that

$$\begin{aligned} r_h(\varphi_N \chi_T) &= \int_T f \varphi_N dx + \int_{\partial T \cap \Gamma_N} (g_N - K \nabla u_h \cdot n) \varphi_N + \int_{\partial T \cap \Gamma_D} \frac{\gamma k_F}{|F|} \varphi_N (g_D - u_h) \\ &\quad - \int_{\partial T \cap \Gamma_D} K \nabla \varphi_N \cdot n (g_D - u_h) ds - \int_{\partial T \cap \mathcal{F}_h^{int}} [K \nabla u_h \cdot n_F] \{\varphi_N \chi_T\}^* ds. \end{aligned}$$

Noting that  $\varphi_N$  vanishes on  $\mathcal{F}_h \setminus \mathcal{F}_N$ , a standard scaling argument yields that:

$$\begin{aligned} |r_h(\varphi_N \chi_T)| &\lesssim h_T \|\pi_T^1 f\|_{0,T} + \sum_{F \in \partial T \cap \mathcal{F}_N \cap \Gamma_N} h_F^{1/2} \|K \nabla u_h \cdot n - \pi_F^1 g_N\|_{0,F} \\ &+ \sum_{F \in \partial T \cap \mathcal{F}_N \cap \Gamma_D} \frac{\gamma k_F}{h_F^{1/2}} \|u_h - \pi_F^1 g_D\|_{0,F} + \sum_{F \in \partial T \cap \Gamma_D} \frac{k_T}{h_F^{1/2}} \|\pi_F^0(u_h - g_D)\|_{0,F} \\ &+ \sum_{F \in \partial T \cap \mathcal{F}_N \cap \mathcal{F}_h^{int}} h_F^{1/2} \bar{\omega}_{F,T} \|[K \nabla u_h \cdot n_F]\|_{0,F}. \end{aligned}$$

238 We next multiply the previous inequality by  $k_T^{-1/2}$  and use that  $k_F = k_T$  on the  
239 Dirichlet sides, and that  $\|\pi_F^0 w\|_{0,F} \leq \|\pi_F^1 w\|_{0,F}$ . Lemma 4.3 yields the result.  $\square$

**4.2. Nonconforming approximation.** The residual is now given by:

$$r_h^*(\cdot) = l_h(\cdot) - \tilde{a}_h^*(u_h, \cdot).$$

240 Thanks to the mixed formulation, we have  $r_h^*(v_h) = 0$  for any  $v_h \in \mathcal{NC}_h^k$  and

$$l_h^*(\theta_h^*, v_h) = r_h^*(v_h) \quad \forall v_h \in \mathcal{DG}_h^k. \quad (4.15)$$

241 Let any  $F \in \mathcal{F}_h^{int}$ . We define  $\theta_F \in \mathcal{M}_h^{k-1}$  by imposing  $(\theta_F)_{|F'} = 0$  for any  
242  $F' \neq F$ , whereas  $(\theta_F)_{|F} \in P^{k-1}$  is given by:

$$b_h^*(\theta_F, \phi_{F,i} \chi_T) = r_h^*(\phi_{F,i} \chi_T), \quad \forall T \in \Delta_F, \quad 0 \leq i \leq k-1. \quad (4.16)$$

The support of  $\phi_{F,i} \in \mathcal{NC}_h^k$  is  $\Delta_F$  so we have that

$$0 = r_h^*(\phi_{F,i}) = \sum_{T \in \Delta_F} r_h^*(\phi_{F,i} \chi_T), \quad 0 \leq i \leq k-1.$$

Furthermore, by definition of the nonconforming space, we also have that

$$\sum_{T \in \Delta_F} b_h^*(\theta_F, \phi_{F,i} \chi_T) = \int_F \theta_F [\phi_{F,i}] ds = 0, \quad 0 \leq i \leq k-1.$$

243 So the system (4.16) is compatible and is equivalent to:

$$\int_F \theta_F \phi_{F,i} ds = \mathfrak{s}_{F,T^*} r_h^*(\phi_{F,i} \chi_{T^*}), \quad 0 \leq i \leq k-1 \quad (4.17)$$

244 where  $T^*$  is the triangle of  $\Delta_F$  with the smallest coefficient  $k$  and  $\mathfrak{s}_{F,T^*} = n_F \cdot n_{T^*}$ .  
245 Writing  $\theta_F \in P^{k-1}(F)$  in the Legendre basis as  $\theta_F = \sum_{j=0}^{k-1} \theta_{F,j} L_j$  yields the unique  
246 solution of (4.17), with  $|F| |\theta_{F,j}| = |r_h^*(\phi_{F,j} \chi_{T^*})|$  for  $0 \leq j \leq k-1$ . In addition, using  
247 that  $k_F^{-1} \leq 2k_{T^*}^{-1}$  we get a robust bound for  $\theta_F$ , similar to the one of Lemma 4.3:

$$\|\theta_F\|_{\mathcal{NC}_h}^2 \lesssim k_F^{-1} |F|^2 \sum_{j=0}^{k-1} \theta_{F,j}^2 \leq 2k_{T^*}^{-1} \sum_{j=0}^{k-1} r_h^*(\phi_{F,j} \chi_{T^*})^2. \quad (4.18)$$

248 **LEMMA 4.5.** *Let  $\theta_h^*$  and  $\theta_F$  be the solutions of (4.15) and (4.16), respectively.*

249 *Then  $\theta_h^* = \sum_{F \in \mathcal{F}_h^{int}} \theta_F$ .*

250 *Proof.* Let  $\bar{\theta}_h := \sum_{F \in \mathcal{F}_h^{int}} \theta_F$ . We show that  $\bar{\theta}_h$  satisfies (4.15), which yields that

251  $\bar{\theta}_h = \theta_h^*$  thanks to the inf-sup condition.

We first consider  $v_h = \phi_j^T \chi_T$ , for any  $T \in \mathcal{T}_h$  and  $0 \leq j \leq \frac{k(k-1)}{2}$ . On the one hand, since this test-function belongs to  $\mathcal{NC}_h^k$ , we have that  $r_h^*(\phi_j^T \chi_T) = 0$ . On the other hand, we also have

$$b_h^*(\bar{\theta}_h, \phi_j^T \chi_T) = \sum_{F \in \mathcal{F}_h^{int}} b_h^*(\theta_F, \phi_j^T \chi_T) = \sum_{F \in (\partial T \cap \mathcal{F}_h^{int})} \mathfrak{s}_{F,T} \int_F \theta_F \phi_j^T ds = 0,$$

252 by using the decomposition of  $\theta_F$  in the Legendre basis of  $P^{k-1}(F)$  and the degrees  
253 of freedom (3.5) of the nodal basis function  $\phi_j^T$ .

Next, we take  $v_h = \phi_{F,i} \chi_T$ , for any  $F \in \mathcal{F}_h$ ,  $T \subset \Delta_F$  and  $0 \leq i \leq k-1$ . If  $F \in \mathcal{F}_h^{int}$ , then we have thanks to (4.16):

$$b_h^*(\bar{\theta}_h, \phi_{F,i} \chi_T) = \sum_{F' \in \mathcal{F}_h^{int}} b_h^*(\theta_{F'}, \phi_{F,i} \chi_T) = b_h^*(\theta_F, \phi_{F,i} \chi_T) = r_h^*(\phi_{F,i} \chi_T).$$

254 Here above, we have used the fact that  $\int_{F'} \theta_{F'} \phi_{F,i} ds = 0$  for  $F' \neq F$ , according to  
255 (3.5). Finally, if  $F \in \mathcal{F}_h^\partial$  then  $v_h \in \mathcal{NC}_h^k$  so  $r_h^*(v_h) = 0$ , and  $b_h^*(\bar{\theta}_h, v_h) = 0$  too.

256 We have thus shown that  $b_h^*(\bar{\theta}_h, v_h) = r_h^*(v_h)$  for any  $v_h \in \mathcal{DG}_h^k$ , so  $\bar{\theta}_h = \theta_h^*$ .  $\square$

## 257 5. Local flux reconstruction.

258 **5.1. Conforming approximation.** Thanks to the definition of the multiplier  
259  $\theta_h$ , we are now able to reconstruct the local flux  $\sigma_h$  belonging to  $H(\text{div}, \Omega)$ . For this  
260 purpose, we use the Raviart-Thomas finite element space  $RT_h^m$ , with  $m = 0$  or  $1$ . We  
261 impose the degrees of freedom of  $\sigma_h$  as follows.

262 On the Neumann boundary, we simply set on any  $F \in \mathcal{F}_h^N$ :

$$\sigma_h \cdot n_F = \pi_h^m g_N. \quad (5.1)$$

263 On the Dirichlet boundary, we set on any  $F \in \mathcal{F}_h^D$ :

$$\int_F \sigma_h \cdot n_F \varphi ds = \int_F \left( K \nabla u_h \cdot n_F - \frac{\gamma k_F}{|F|} (u_h - g_D) \right) \varphi ds, \quad \forall \varphi \in P^m(F), \quad (5.2)$$

264 which translates into  $\sigma_h \cdot n_F = K \nabla u_h \cdot n_F - \frac{\gamma k_F}{|F|} \pi_F^m (u_h - g_D)$ . On a interior side  
265  $F \in \mathcal{F}_h^{int}$  we impose:

$$\int_F \sigma_h \cdot n_F \varphi ds = \int_F \{K \nabla u_h \cdot n_F\} \varphi ds - b_F(\theta_h, \varphi), \quad \forall \varphi \in P^m(F). \quad (5.3)$$

266 The previous relations allow to uniquely define  $\sigma_h \cdot n_F$  in  $P^m(F)$  for any  $F \in \mathcal{F}_h$ .

267 If  $m = 1$ , then we also define interior degrees of freedom on any  $T \in \mathcal{T}_h$  as follows:

$$\int_T \sigma_h \cdot r dx = \int_T K \nabla u_h \cdot r dx - \int_{\partial T \cap \Gamma_D} (u_h - g_D) K r \cdot n ds, \quad \forall r \in (P^0(T))^2. \quad (5.4)$$

268 Similarly to [10], we can then prove the following statement.

269 **THEOREM 5.1.** *The flux  $\sigma_h$  satisfies the following conservation property:*

$$(\text{div} \sigma_h)|_T = -\pi_T^m f, \quad \forall T \in \mathcal{T}_h. \quad (5.5)$$

**5.2. Nonconforming approximation.** We are now able to reconstruct the local flux  $\sigma_h^*$  in  $H(\text{div}, \Omega)$ , more precisely in the Raviart-Thomas finite element space  $RT_h^{k-1}$ . On the sides, its degrees of freedom are given by:

$$\begin{aligned} \forall F \in \mathcal{F}_h^N, \quad \sigma_h^* \cdot n_F &= \pi_F^{k-1} g_N, \\ \forall F \in \mathcal{F}_h^D, \quad \sigma_h^* \cdot n_F &= \pi_F^{k-1} \left( K \nabla u_h^* \cdot n_F - \frac{\gamma_F^{k_F}}{|F|} (u_h^* - g_D) \right), \\ \forall F \in \mathcal{F}_h^{\text{int}}, \quad \sigma_h^* \cdot n_F &= \pi_F^{k-1} \{ K \nabla u_h^* \cdot n_F \} - \theta_h^*. \end{aligned} \quad (5.6)$$

The interior degrees of freedom are defined as follows, for any  $T \in \mathcal{T}_h$ ,  $r \in (P^{k-2}(T))^2$ :

$$\int_T \sigma_h^* \cdot r \, dx = \int_T K \nabla u_h^* \cdot r \, dx - \int_{\partial T \cap \mathcal{F}_h^D} (u_h^* - g_D) K r \cdot n \, ds, \quad \forall r \in (P^{k-2}(T))^2. \quad (5.7)$$

**THEOREM 5.2.** *The flux  $\sigma_h^*$  satisfies the following conservation property:*

$$(\text{div} \sigma_h^*)|_T = -\pi_T^{k-1} f, \quad \forall T \in \mathcal{T}_h.$$

*Proof.* Let  $T \in \mathcal{T}_h$ ,  $p \in P^{k-1}(T) \subset V_k(T)$  and let  $v := p\chi_T \in \mathcal{DG}_h^k$ . We start from the integration by parts formula:

$$-\int_T (\text{div} \sigma_h^*) p \, dx = \int_T \sigma_h^* \cdot \nabla v \, dx - \int_{\partial T} \sigma_h^* \cdot n_T v \, ds. \quad (5.8)$$

From (5.6) and (5.7) with  $r := \nabla v$ , we get using  $v|_F n_T = [v]_F n_F$  that:

$$\begin{aligned} \int_F \sigma_h^* \cdot n_T v \, ds &= \int_F \{ K \nabla u_h^* \cdot n_F \} [v] \, ds - \int_F \theta_h^* [v] \, ds, \quad \forall F \in \partial T \cap \mathcal{F}_h^{\text{int}}, \\ \int_F \sigma_h^* \cdot n_T v \, ds &= \int_F K \nabla u_h^* \cdot n_F v \, ds - \int_F \frac{\gamma_F^{k_F}}{|F|} (u_h^* - g_D) v \, ds, \quad \forall F \in \partial T \cap \mathcal{F}_h^D, \\ \int_F \sigma_h^* \cdot n_T v \, ds &= \int_F g_N v \, ds, \quad \forall F \in \partial T \cap \mathcal{F}_h^N, \\ \int_T \sigma_h^* \cdot \nabla v \, dx &= \int_T K \nabla u_h^* \cdot \nabla v \, dx - \int_{\partial T \cap \mathcal{F}_h^D} (u_h^* - g_D) K \nabla v \cdot n \, ds. \end{aligned}$$

Replacing in (5.8) we obtain:

$$\begin{aligned} -\int_T (\text{div} \sigma_h^*) p \, dx &= \int_T K \nabla u_h^* \cdot \nabla v \, dx - \int_{\partial T \cap \mathcal{F}_h^D} (K \nabla v \cdot n u_h^* + K \nabla u_h^* \cdot n v) \, ds \\ &\quad + \int_{\partial T \cap \mathcal{F}_h^D} \frac{\gamma_F^{k_F}}{|F|} (u_h^* - g_D) v \, ds - \int_{\partial T \cap \mathcal{F}_h^{\text{int}}} \pi_F^{k-1} \{ K \nabla u_h^* \cdot n_F \} [v] \, ds \\ &\quad + \sum_{F \in \partial T \cap \mathcal{F}_h^{\text{int}}} \int_F \theta_h^* [v] \, ds + \int_{\partial T \cap \mathcal{F}_h^D} g_D K \nabla v \cdot n \, ds - \int_{\partial T \cap \mathcal{F}_h^N} g_N v \, ds. \end{aligned}$$

Noting that  $\int_{\partial T \cap \mathcal{F}_h^{\text{int}}} \pi_F^{k-1} \{ K \nabla v \cdot n_F \} [u_h^*] \, ds = 0$  because  $u_h^* \in \mathcal{NC}_h^k$ , we further get

$$-\int_T (\text{div} \sigma_h^*) p \, dx = \tilde{a}_h^*(u_h^*, v) + b_h^*(\theta_h^*, v) - l_h(v) + \int_T f v \, dx = \int_T f p \, dx,$$

since  $(u_h^*, \theta_h^*)$  is solution of the mixed formulation (3.2). This ends the proof.  $\square$



**6. Application to a posteriori error analysis.** We only consider here the  $P^1$ -continuous approximation. For the sake of simplicity, we set  $f_h = \pi_T^m f$  and  $g_h = \pi_F^m g_N$ , and we also assume that  $g_D$  is a piecewise  $P^1$ -continuous function. Let  $\tau_h = K^{-1/2}(\sigma_h - K\nabla u_h)$ . We introduce the local error estimators:

$$\begin{aligned}\eta_T &= \|K^{-1/2}(\sigma_h - K\nabla u_h)\|_{0,T} = \|\tau_h\|_{0,T}, \quad \forall T \in \mathcal{T}_h, \\ \eta_F &= \left( \int_F \frac{k_F}{|F|} (u_h - g_D)^2 ds \right)^{1/2}, \quad \forall F \in \mathcal{F}_h^D,\end{aligned}$$

and the corresponding global error estimators

$$\eta = \left( \sum_{T \in \mathcal{T}_h} \eta_T^2 \right)^{1/2} = \|\tau_h\|_{0,\Omega}, \quad \eta_D = \left( \sum_{F \in \mathcal{F}_h^D} \eta_F^2 \right)^{1/2}.$$

Let also the following higher order term, representing the data approximation:

$$\epsilon(\Omega)^2 = \sum_{T \in \mathcal{T}_h} \frac{h_T^2}{k_T} \|f - f_h\|_{0,T}^2 + \sum_{F \in \mathcal{F}_h^N} \frac{h_F}{k_F} \|g_N - g_h\|_{0,F}^2.$$

**6.1. Reliability.** LEMMA 6.1. *Let  $\sigma_h$  be given by the equations (5.1)-(5.4) and let  $u_h$  the solution of the weak formulation (3.1). Then we have the following estimate:*

$$|u - u_h|_{1,K} \leq \eta + C_D \eta_D + C\epsilon(\Omega) \quad (6.1)$$

where  $C_D \simeq \max_{N \in \mathcal{N}_h^D} \{C_N\}$  and  $C_N$  is defined in (4.5).

*Proof.* Let  $\varphi \in V^{g_D}$  the unique solution of

$$\int_{\Omega} K \nabla \varphi \cdot \nabla v \, dx = \int_{\Omega} K \nabla u_h \cdot \nabla v \, dx, \quad \forall v \in V^0. \quad (6.2)$$

By the triangle inequality, we have

$$|u - u_h|_{1,K} \leq |u - \varphi|_{1,K} + |\varphi - u_h|_{1,K}, \quad (6.3)$$

where

$$\begin{aligned}|u - \varphi|_{1,K}^2 &= \int_{\Omega} K^{1/2} \nabla(u - \varphi) \cdot (K^{1/2} \nabla u - K^{-1/2} \sigma_h) \, dx \\ &\quad + \int_{\Omega} K^{1/2} \nabla(u - \varphi) \cdot \tau_h \, dx + \int_{\Omega} K^{1/2} \nabla(u - \varphi) \cdot K^{1/2} \nabla(u_h - \varphi) \, dx \\ &\leq |u - \varphi|_{1,K} \|\tau_h\|_{\Omega} + \int_{\Omega} \nabla(u - \varphi) \cdot (K \nabla u - \sigma_h) \, dx,\end{aligned}$$

by testing (6.2) with  $v := u - \varphi \in V^0$ . Since  $K \nabla u - \sigma_h \in H(\text{div}, \Omega)$  and  $u - \varphi \in H^1(\Omega)$ , integration by parts in the last term yields, thanks to Lemma 5.1, that:

$$\int_{\Omega} \nabla(u - \varphi) \cdot (K \nabla u - \sigma_h) \, dx = \int_{\Omega} (f - f_h)(u - \varphi) \, dx + \int_{\Gamma_N} (g_N - g_h)(u - \varphi) \, ds.$$

The right-hand side term is classically bounded by  $C|u - \varphi|_{1,K}\epsilon(\Omega)$ . Thus, we have so far proved that

$$|u - \varphi|_{1,K} \leq \eta + C\epsilon(\Omega).$$

We next bound the remaining term in (6.3),  $|u_h - \varphi|_{1,K}$ . From (6.2), we have

$$|\varphi - u_h|_{1,K} = \inf_{v \in V^{g_D}} |v - u_h|_{1,K}$$

so it is sufficient to build  $v \in V^{g_D}$  such that  $|v - u_h|_{1,K}$  is bounded by  $\eta_D$ . We choose  $v \in \mathcal{C}_h^1$  defined by

$$v(N) = u_h(N), \quad \forall N \in \mathcal{N}_h^{int} \cup \mathcal{N}_h^N, \quad v(N) = g_D(N) \quad \forall N \in \mathcal{N}_h^D.$$

For simplicity of notation, we set  $\mathcal{D} = \{T \in \mathcal{T}_h : T \cap \bar{\Gamma}_D \neq \emptyset\}$ . Then we have

$$|v - u_h|_{1,K}^2 = \sum_{T \in \mathcal{D}} \int_T K \nabla(v - u_h) \cdot \nabla(v - u_h) dx \lesssim \sum_{T \in \mathcal{D}} \sum_{N \in \mathcal{N}_T} k_T (v - u_h)^2(N).$$

For a triangle  $T \in \mathcal{D}$  which has a side  $F \in \mathcal{F}_h^D$ , one has that  $k_F = k_T$  and

$$\sum_{N \in \mathcal{N}_T} k_T (v - u_h)(N)^2 = \sum_{N \in \mathcal{N}_F} k_F (g_D - u_h)^2(N) \simeq \eta_F^2.$$

Meanwhile, for  $T \in \mathcal{D}$  which has only a node  $N \in \mathcal{N}_h^D$ , one can bound  $k_T$  by  $\mathcal{C}_N^2 k_F$ , where  $F \in \mathcal{F}_h^D \cap \mathcal{F}_N$ . Hence, we finally get that

$$|v - u_h|_{1,K} \leq \mathcal{C}_D \eta_D$$

and the announced bound follows from (6.3).  $\square$

**REMARK 1.** For  $m = 1$ , the definition of  $\sigma_h$  on a Dirichlet side  $F \subset \partial T$  together with the Cauchy-Schwarz inequality yield that  $\eta_F \leq h_F^{1/2} \gamma^{-1} \|\tau_h \cdot n\|_{0,F} \lesssim \gamma^{-1} \|\tau_h\|_{0,T}$ , so one can bound  $\eta_D$  by  $\eta$ .

**6.2. Efficiency.** **LEMMA 6.2.** Let  $T \in \mathcal{T}_h$ . We have the following estimate:

$$\begin{aligned} \eta_T &\lesssim \mathcal{C}_T \sum_{T' \in \Delta_T} \left( \frac{h_{T'}}{k_{T'}^{1/2}} \|f_h\|_{0,T'} + \sum_{F \in \partial T' \cap \Gamma_D} \frac{k_F^{1/2}}{h_F^{1/2}} \|u_h - g_D\|_{0,F} \right. \\ &\quad \left. + \sum_{F \in \partial T' \setminus \partial \Delta_T} \frac{\bar{\omega}_{F,T'} h_F^{1/2}}{k_{T'}^{1/2}} \|[K \nabla u_h \cdot n_F]\|_{0,F} \right) + \sum_{F \in \partial T \cap \Gamma_N} \frac{h_F^{1/2}}{k_T^{1/2}} \|K \nabla u_h \cdot n - g_h\|_{0,F} \end{aligned}$$

where  $\mathcal{C}_T = \max_{N \in \mathcal{N}_T} \mathcal{C}_N$  and  $\Delta_T = \{T' \in \mathcal{T}_h; \partial T' \cap \partial T \neq \emptyset\}$ .

*Proof.* Using the degrees of freedom of the Raviart-Thomas space  $RT^m(T)$ , we have the following well-known inequality for  $\tau_h = K^{-1/2}(\sigma_h - K \nabla u_h)$ :

$$\|\tau_h\|_{0,T} \lesssim \frac{1}{k_T^{1/2}} \|\pi_T^{m-1}(\sigma_h - K_T \nabla u_h)\|_{0,T} + \sum_{F \in \partial T} \frac{h_F^{1/2}}{k_T^{1/2}} \|(\sigma_h - K_T \nabla u_h) \cdot n_F\|_{0,F}. \quad (6.4)$$

We next bound the right-hand-side term using the definition of the flux, that is relations (5.1)-(5.4). For  $F \in \partial T \cap \Gamma_N$ , we immediately have that:

$$h_F^{1/2} k_T^{-1/2} \|(\sigma_h - K_T \nabla u_h) \cdot n_F\|_{0,F} = h_F^{1/2} k_T^{-1/2} \|K_T \nabla u_h \cdot n - g_h\|_{0,F}, \quad (6.5)$$

293 whereas for  $F \in \partial T \cap \Gamma_D$  we have with  $k_F = k_T$ :

$$h_F^{1/2} k_T^{-1/2} \|(\sigma_h - K_T \nabla u_h) \cdot n_F\|_{0,F} = \gamma h_F^{-1/2} k_F^{1/2} \|\pi_F^m(u_h - g_D)\|_{0,F}. \quad (6.6)$$

For  $F \in \partial T \cap \mathcal{F}_h^{int}$ , we use that  $\{a\} - a^- = -\omega^+[a]$  and  $\{a\} - a^+ = \omega^-[a]$  and we get, for any  $\varphi \in P^m(F)$ :

$$\int_F (\sigma_h - K_T \nabla u_h) \cdot n_F \varphi \, ds = -(n_F \cdot n_T) \bar{\omega}_{F,T} \int_F [K \nabla u_h \cdot n_F] \varphi \, ds - b_F(\theta_h, \varphi).$$

Taking  $\varphi = (\sigma_h - K_T \nabla u_h) \cdot n_F$  as test-function and using that  $k_F \leq k_T$ , we get

$$\begin{aligned} h_F^{1/2} k_T^{-1/2} \|(\sigma_h - K_T \nabla u_h) \cdot n_F\|_{0,F} &\lesssim h_F^{1/2} k_T^{-1/2} \bar{\omega}_{F,T} \| [K \nabla u_h \cdot n_F] \|_{0,F} \\ &\quad + \left( \sum_{N \in \mathcal{N}_F} |F| k_F^{-1} (\theta_N)_{|F}^2(N) \right)^{1/2}. \end{aligned}$$

294 Let  $\mathcal{D}_F = \bigcup_{N \in \mathcal{N}_F} \omega_N = \{T' \in \mathcal{T}_h; \partial T' \cap \bar{F} \neq \emptyset\}$  and  $\mathcal{C}_F = \max_{N \in \mathcal{N}_F} \mathcal{C}_N$ . Thanks to

295 Theorem 4.4, we deduce that:

$$\begin{aligned} &h_F^{1/2} k_T^{-1/2} \|(\sigma_h - K \nabla u_h) \cdot n_F\|_{0,F} \\ &\lesssim \mathcal{C}_F \sum_{T' \in \mathcal{D}_F} \left( \frac{h_{T'}}{k_{T'}^{1/2}} \|f_h\|_{0,T'} + \sum_{F' \in \partial T' \setminus \partial \mathcal{D}_F} \frac{\bar{\omega}_{F',T'} h_{F'}^{1/2}}{k_{T'}^{1/2}} \| [K \nabla u_h \cdot n_{F'}] \|_{0,F'} \right. \\ &\quad \left. + \sum_{F' \in \partial T' \cap \Gamma_N} \frac{h_{F'}^{1/2}}{k_{T'}^{1/2}} \|K_{T'} \nabla u_h \cdot n - g_h\|_{0,F'} + \sum_{F' \in \partial T' \cap \Gamma_D} \frac{k_{F'}^{1/2}}{h_{F'}^{1/2}} \|u_h - g_D\|_{0,F'} \right). \end{aligned} \quad (6.7)$$

296 Concerning the interior degrees of freedom (for  $m = 1$ ), taking  $r = \pi_T^0(\sigma_h - K_T \nabla u_h)$   
297 in (5.4) yields that

$$k_T^{-1/2} \|\pi_T^0(\sigma_h - K \nabla u_h)\|_{0,T} \lesssim \sum_{F \in \partial T \cap \Gamma_D} h_F^{-1/2} k_F^{1/2} \|\pi_F^0(u_h - g_D)\|_{0,F}. \quad (6.8)$$

Gathering together (6.5), (6.6), (6.7) and (6.8) in (6.4) and putting

$$\mathcal{C}_T := \max_{F \in \partial T} \mathcal{C}_F = \max_{N \in \mathcal{N}_T} \mathcal{C}_N, \quad \Delta_T := \bigcup_{F \in \partial T \cap \mathcal{F}_h^{int}} \mathcal{D}_F = \{T' \in \mathcal{T}_h; \partial T' \cap \partial T \neq \emptyset\},$$

298 we obtain the desired bound.  $\square$

299 For any  $T \in \mathcal{T}_h$  and  $F \in \partial T \cap \mathcal{F}_h^N$ , we have thanks to Verfurth's argument [24]:

$$\begin{aligned} &\frac{h_T}{k_T^{1/2}} \|f_h\|_{0,T} \lesssim |u - u_h|_{1,T,K} + \frac{h_T}{k_T^{1/2}} \|f - f_h\|_{0,T}, \\ &\frac{h_F^{1/2}}{k_F^{1/2}} \|K \nabla u_h \cdot n - g_h\|_{0,F} \lesssim |u - u_h|_{1,T,K} + \frac{h_T}{k_T^{1/2}} \|f - f_h\|_{0,T} + \frac{h_F^{1/2}}{k_F^{1/2}} \|g_N - g_h\|_{0,F}. \end{aligned} \quad (6.9)$$

LEMMA 6.3. *Let  $T \in \mathcal{T}_h$  and  $F \in \partial T \cap \mathcal{F}_h^{int}$ . Then we have:*

$$\frac{h_F^{1/2} \bar{\omega}_{F,T}}{k_T^{1/2}} \| [K \nabla u_h \cdot n_F] \|_{0,F} \lesssim |u - u_h|_{1,\Delta_F,K} + \sum_{T' \subset \Delta_F} \frac{h_{T'}}{k_{T'}^{1/2}} \|f - f_h\|_{0,T'}.$$

*Proof.* We start from the next estimate, obtained again by means of Verfurth's argument:

$$h_F^{1/2} \| [K \nabla u_h \cdot n_F] \|_{0,F} \lesssim \sum_{T' \subset \Delta_F} \| K \nabla (u - u_h) \|_{0,T'} + \sum_{T' \subset \Delta_F} h_{T'} \| f - f_h \|_{0,T'}.$$

We multiply the inequality by  $\bar{\omega}_{F,T} k_T^{-1/2}$  and we note that for  $T' = T$ , we obviously have  $(\bar{\omega}_{F,T} k_T^{1/2}) k_T^{-1/2} = \bar{\omega}_{F,T} = 1$ , whereas for  $T' \neq T$  we get, thanks to the definition of  $\bar{\omega}_{F,T}$  and to the mean inequality,

$$\frac{\bar{\omega}_{F,T} k_T^{1/2}}{k_T^{1/2}} = \frac{k_T^{1/2} k_{T'}^{1/2}}{k_T + k_{T'}} \leq \frac{1}{2}.$$

This finally yields the announced estimate.  $\square$

Combining Lemmas 6.2 and 6.3 and estimates (6.9), we have the following result.

**THEOREM 6.4 (Efficiency).** *We have the following local efficiency bound:*

$$\eta_T \lesssim \mathcal{C}_T (\|u - u_h\|_{\Delta_T} + \epsilon(\Delta_T)),$$

with  $\mathcal{C}_T = 1$  if the coefficient  $K$  is quasi-monotone.

Note that by definition of the energy norm, one also has that  $\eta_F \leq \|u - u_h\|_{\Delta_F}$  for any Dirichlet side  $F$ .

**7. Numerical tests.** We present some numerical experiments carried out for the  $P^1$ -continuous approximation. For the stabilisation parameter in Nitsche's method, we set  $\gamma = 50$ . As regards the refinement strategy, we use the Dörfler marking strategy and the refinement rate is set to be 10%. In the adaptive mesh refinement (AMR) procedure, the marking percent is set to be 20%.

**EXAMPLE 7.1 (The Ellipse Example).** *Let  $\Omega = [-1, 1]^2$  and let the ellipse centered at the origin, with width  $2a$  and height  $2b$ , of equation  $\rho = 1$ , where  $\rho = \sqrt{\frac{x^2}{a^2} + \frac{y^2}{b^2}}$ . Here, we take  $a = \frac{\pi}{6.18}$  and  $b = 1.5a$ . The exact solution is given by*

$$u(x, y) = \begin{cases} \frac{1}{k_1} \rho^p & \text{if } \rho \leq 1 \\ \frac{1}{k_2} \rho^p + \frac{1}{k_1} - \frac{1}{k_2} & \text{if } \rho > 1 \end{cases},$$

where  $p = 5$  and the diffusion coefficients in the two sub-domains are  $k_1 = 1.0$  and  $k_2 = 10k_1$ , respectively.

The stopping criteria in the AMR procedure is that the total number  $N$  of degrees of freedom is less than 15000. The initial and final mesh generated by  $\eta_K$  are provided in Figure 7.1.

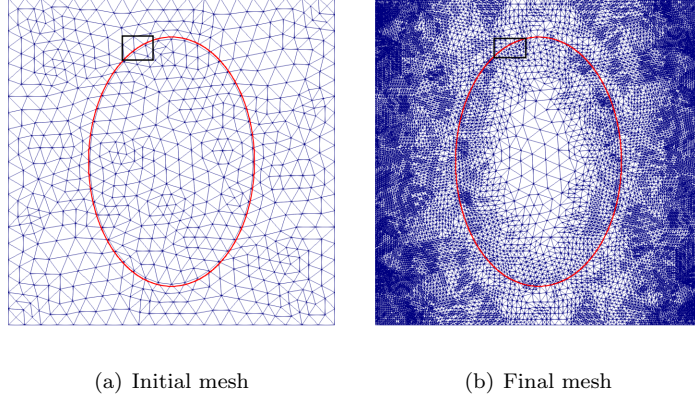


Fig. 7.1: (Example 7.1) Initial and final meshes

315 In Figure 7.2, we show the process of boundary snapping. When an element is  
 316 refined, we use the longest edge refinement method, i.e., we add the mid-point of the  
 317 longest edge to the vertices and form two sub-triangles. If the longest edge has two  
 318 endpoints lying on the interface, we will adjust the newly added vertex to the interface  
 319 after the refinement if such a movement does not deteriorate the mesh regularity.

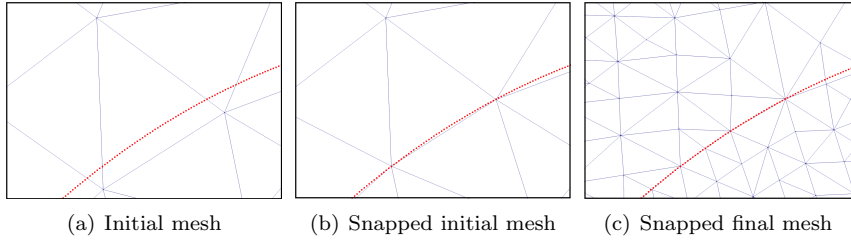


Fig. 7.2: (Example 7.1) A zoomed interface snapping from Figure 7.1

320 In Figure 7.3, we observe optimal convergence rates for the error, the residual-  
 321 based and the recovered flux-based estimators. However, the efficiency index (i.e. the  
 322 ratio between the estimator and the error) of  $\eta$  is more accurate than that of  $\eta_{res}$ .

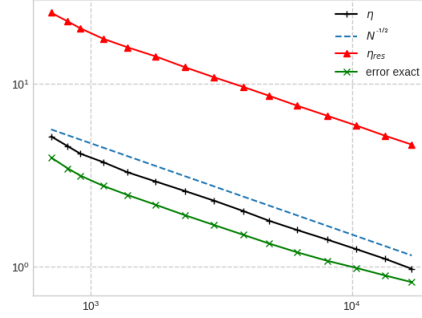


Fig. 7.3: (Example 7.1) Error convergence

EXAMPLE 7.2 (The L-shaped domain). *We now consider the L-shaped domain test, see for instance [26]. The domain is  $\Omega = [-5, 5] \times [-5, 5] \setminus [0, 5] \times [-5, 0]$  and it presents again an interface, the circle centered at origin and of radius  $\rho_0 = 2\sqrt{2}$ . The exact solution is given in polar coordinates  $(\rho, \theta)$  by:*

$$u(\rho, \theta) = \begin{cases} \rho^{2/3} \sin \frac{2\theta}{3}, & \text{if } \rho \leq \rho_0 \\ \rho_0^{2/3} \sin \frac{2\theta}{3} + \frac{2}{3\mu} \rho_0^{-1/3} \sin \frac{2\theta}{3} (\rho - \rho_0) & \text{otherwise} \end{cases},$$

whereas the diffusion coefficient  $k$  is defined as follows:

$$k(\rho) = \begin{cases} 1 & \text{if } \rho \leq \rho_0 \\ \mu & \text{otherwise} \end{cases}.$$

323 As stopping criteria in the AMR procedure, we now impose that the total number  
 324 of degrees of freedom is less than 45000. The curved interface is treated as in the  
 325 previous example, by snapping the mesh. Figure 7.4 shows a sequence of adapted  
 326 meshes, while in Figure 7.5 one can see the convergence rates obtained for different  
 327 values of  $\mu$ , from 5 to 10000. As expected from the theoretical results, we numerically  
 328 retrieve the robustness with respect to the jump of the diffusion coefficient.

EXAMPLE 7.3 (The Kellogg test). *We now consider the well-known checkerboard example, originally proposed by Kellogg [27]. Here, the line discontinuity of the diffusion coefficients meets the singularity of the solution. In addition, the coefficients are not quasi-monotone around the origin. The domain is  $\Omega = [-1, 1]^2$ , with two intersecting interfaces given by the lines  $y = 0$  and  $x = 0$ . The diffusion coefficient is piecewise constant in each of the four sub-domains and is defined as follows:*

$$k(x, y) = \begin{cases} \kappa, & \text{if } xy \geq 0 \\ 1, & \text{otherwise} \end{cases}.$$

The exact solution is given by  $u(r, \theta) = r^\delta \mu(\theta)$ , with  $(r, \theta)$  the polar coordinates centered at the origin and

$$\mu(\theta) = \begin{cases} \cos((\frac{\pi}{2} - \sigma)\delta) \cos((\theta - \frac{\pi}{2} + \rho)\delta), & 0 \leq \theta \leq \frac{\pi}{2} \\ \cos(\rho\delta) \cos((\theta - \pi + \sigma)\delta), & \frac{\pi}{2} \leq \theta \leq \pi \\ \cos(\sigma\delta) \cos((\theta - \pi - \rho)\delta) & \pi \leq \theta \leq \frac{3\pi}{2} \\ \cos((\frac{\pi}{2} - \rho)\delta) \cos((\theta - \frac{3}{2}\pi - \sigma)\delta) & \frac{3\pi}{2} \leq \theta \leq 2\pi \end{cases}.$$

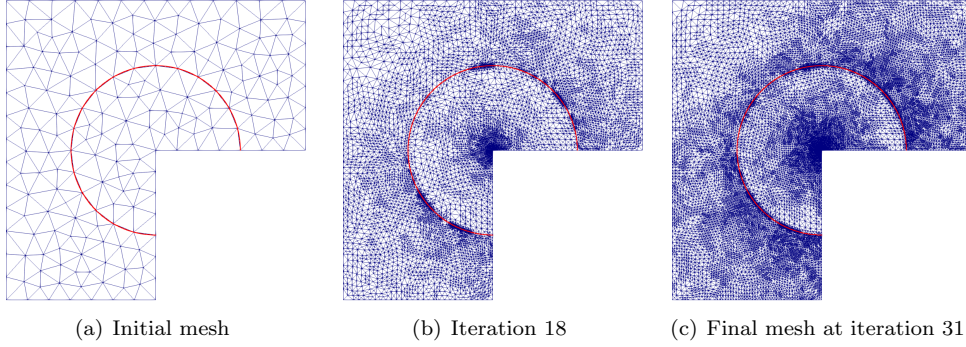


Fig. 7.4: (Example 7.2) Adaptive meshes

The solution has an infinite derivative at the origin and belongs to  $H^{1+s}(\Omega)$  for any  $s < \delta$ . The numbers  $\delta$ ,  $\sigma$ ,  $\rho$  and  $\kappa$  are related by some nonlinear relations. As in [28], we take  $\delta = 0.1$ , which yields  $\sigma = -14.92256510455152$ ,  $\rho = \frac{\pi}{4}$  and  $\kappa = 161.4476387975881$ .

As regards the AMR procedure, the stopping criteria is now that the relative error is less than 1%, which leads to 131 iterations. We present in Figure 7.6 a sequence of adapted meshes, starting from an initial mesh consisting of 8 triangles. One can see that the refinement takes place near the origin, as expected. The optimal convergence rates for the error and the estimators  $\eta$  and  $\eta_{res}$  are shown in Figure 7.7. Again, the efficiency index of  $\eta$  is asymptotically more accurate than that of  $\eta_{res}$ .

EXAMPLE 7.4 (The Battery Problem). Finally, we consider a problem attributed to I. Babuska, which can be found in [29], [30]; it models heat conduction in a battery with non-homogeneous materials. The domain is the rectangle  $\Omega = [0, 8.4] \times [0, 24]$  shown in Figure 7.8. The numbered regions show the areas of different materials; the location of the line segments that separate the regions can be found in [30].

The problem features a piecewise constant diffusion tensor  $K = \begin{pmatrix} k_1 & 0 \\ 0 & k_2 \end{pmatrix}$  and mixed boundary conditions of Fourier-Robin type,  $K \nabla u \cdot n + cu = g$  on  $\partial\Omega$ . Therefore, we have modified accordingly the discrete weak formulation and defined the boundary degrees of freedom  $\sigma_h \cdot n$  as  $\pi_h^m(g - cu_h)$ . The definitions of the parameters  $\omega^\pm$  and  $k_F$  in the tensor case is the same as in [25, 5]. The constants  $k_1$ ,  $k_2$  and  $f$  for each region are given in Table 7.1. The boundary coefficients  $c$  and  $g$  are taken as follows:  $c = g = 0$  on the left,  $c = 1$  and  $g = 3$  on the top,  $c = g = 2$  on the right, and finally,  $c = 3$  and  $g = 1$  on the bottom.

$k$	$k_1$	$k_2$	$f$
1	25	25	0
2	7	0.8	1
3	5	0.0001	1
4	0.2	0.2	0
5	0.05	0.05	0

Table 7.1: (Example 7.4) The piecewise constant coefficient function  $K$

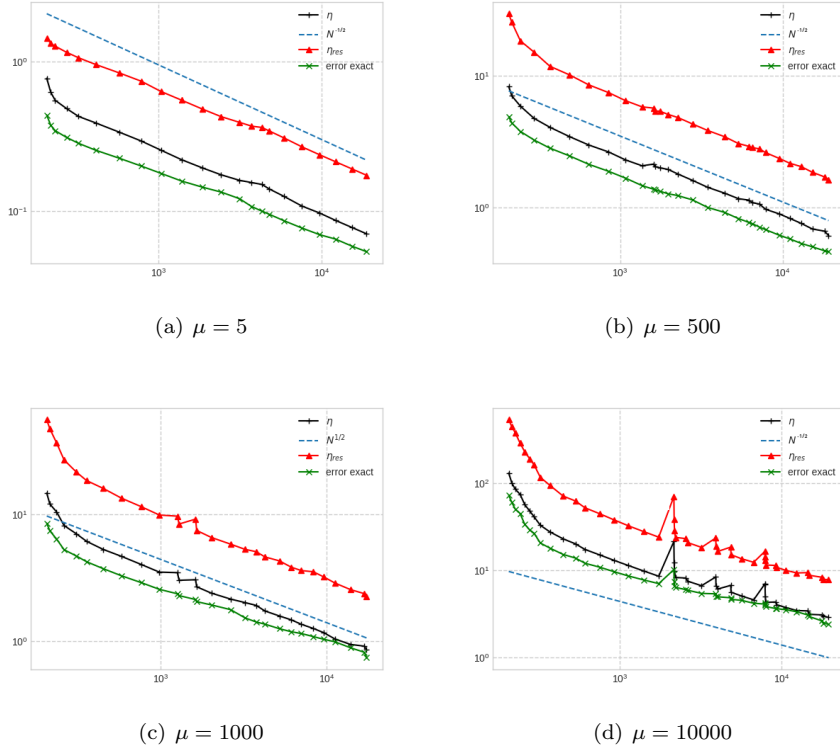
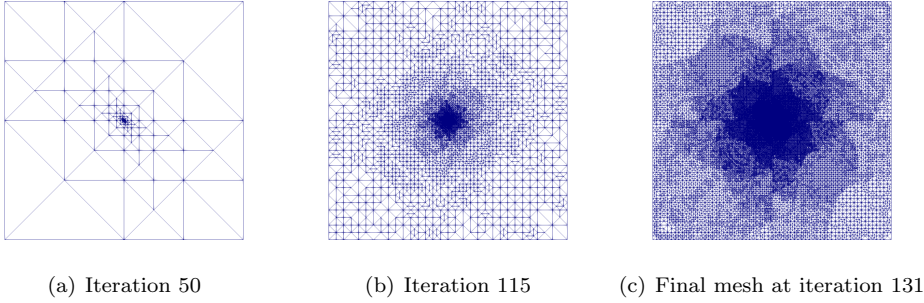
Fig. 7.5: (Example 7.2) Error convergence for different values of  $\mu$ 

Fig. 7.6: (Example 7.3) Adaptive meshes

The exact solution is not known and has singularities at the points where three or more materials meet. For any  $\varepsilon > 0$ , there exists coefficients such that the solution is in  $H^{1+\varepsilon}(\Omega)$ ; for the given set of coefficients,  $\varepsilon$  is about  $1/2$ .

We show in Figure 7.8 a sequence of adapted meshes. Figure 7.9 illustrates the interest of adaptive versus uniform mesh refinement. Besides the gain in the number



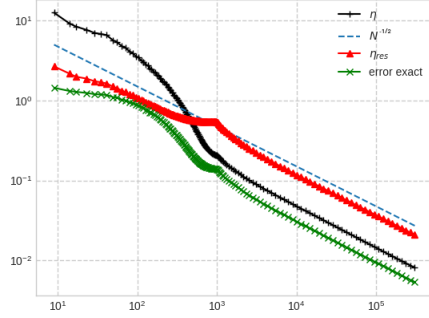


Fig. 7.7: (Example 7.3) Error convergence

357 of degrees of freedom and in computational time, the AMR procedure yields optimal  
 358 convergence rate  $O(h)$  whereas the uniform refinement only yields  $O(h^{1/2})$ .

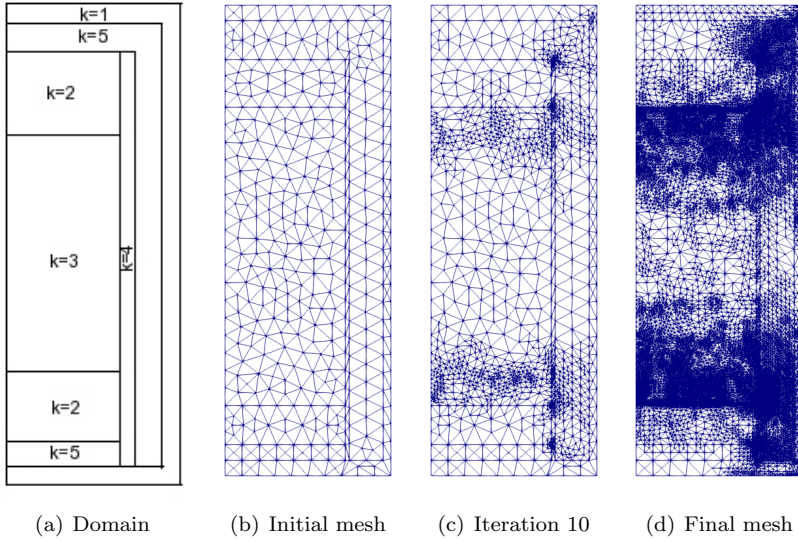


Fig. 7.8: (Example 7.4) sub-domains and adapted meshes

359 **8. Appendix: Proof of Lemma 3.3.** *Proof.* The proof follows the ideas of [10]  
 360 for the Poisson equation. Let  $\mu_h \in \mathcal{M}_h$ . The idea is to construct  $v_h \in \mathcal{D}_h^1$  associated  
 361 to  $\mu_h$  and satisfying

$$b_h(\mu_h, v_h) \gtrsim \|\mu_h\|_{\mathcal{M}_h}^2, \quad \|v_h\|_h \lesssim C_K \|\mu_h\|_{\mathcal{M}_h}. \quad (8.1)$$

362 The construction of  $v_h$  is done patch-wise. We look for  $v_h = \sum_{N \in \mathcal{N}_h^{int}} v_N$  with  
 363  $v_N$  defined on  $\omega_N$ . Let  $N \in \mathcal{N}_h^{int}$  and let us define  $v_N$ , piecewise  $P^1$  and discontinuous  
 364 on  $\omega_N$ , by imposing its values at the nodes of each triangle  $T \in \omega_N$  as follows.

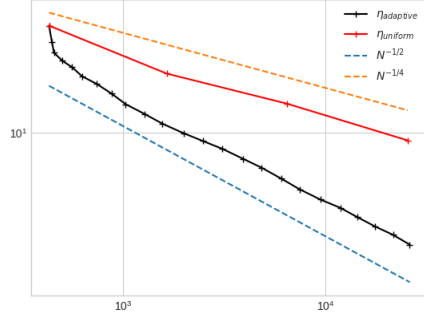


Fig. 7.9: (Example 7.4) Error convergence for adaptive and uniform refinements

At a node  $M \neq N$  belonging to a side  $F \in \mathcal{F}_N$  with  $\{F\} = \partial T^+ \cap \partial T^-$ , we set

$$(v_N)_{|T^\pm}(M) = 0 \quad \text{if } M \in \mathcal{N}_h^{int}.$$

365 If  $M \in \mathcal{N}_h^\partial$ , then we set

$$(v_N)_{|T^-}(M) = \delta_F |F| \mu_h|_F(M), \quad (v_N)_{|T^+}(M) = (\delta_F - 1) |F| \mu_h|_F(M), \quad (8.2)$$

where  $\delta_F = 1$  if  $k_{T^-} \leq k_{T^+}$  and  $\delta_F = 0$  otherwise. This ensures that the definition of  $v_N$  is local and that

$$[v_N]_F(M) = 0 \quad \text{if } M \in \mathcal{N}_h^{int}, \quad [v_N]_F(M) = |F| \mu_h|_F(M) \quad \text{if } M \in \mathcal{N}_h^\partial.$$

366 Furthermore, one has that

$$k_{T^-} \delta_F^2 \leq 2k_F, \quad k_{T^+} (\delta_F - 1)^2 \leq 2k_F. \quad (8.3)$$

367 At the node  $N$ , we impose:

$$[v_N]_F(N) = |F| \mu_h|_F(N), \quad \forall F \in \mathcal{F}_N. \quad (8.4)$$

Thanks to the constraint imposed in the space  $\mathcal{M}_h$ , the linear system (8.4) is compatible, because we have:

$$\forall N \in \mathcal{N}_h^{int}, \quad \sum_{F \in \mathcal{F}_N} \mathfrak{s}_{N,F} [v_N]_F = \sum_{F \in \mathcal{F}_N} \mathfrak{s}_{N,F} |F| \mu_h|_F(N) = 0.$$

The construction of  $v_h$  yields that for any  $F \in \mathcal{F}_h^{int}$  of vertices  $N$  and  $M$ , one has

$$[v_h]_F = [v_N]_F + [v_M]_F = |F| \mu_h|_F,$$

which yields

$$b_h(\mu_h, v_h) = \sum_{F \in \mathcal{F}_h^{int}} \frac{|F|^2 k_F}{2} \sum_{N \in \mathcal{N}_F} \mu_h|_F(N)^2 \simeq \int_{\mathcal{F}_h^{int}} |F| k_F \mu_h^2 = \|\mu_h\|_{\mathcal{M}_h}^2,$$

as well as

$$\sum_{F \in \mathcal{F}_h^{int}} \int_F k_F |F|^{-1} [v_h]^2 ds \lesssim \|\mu_h\|_{\mathcal{M}_h}^2.$$

Meanwhile, for a boundary side  $F \in \mathcal{F}_h^\partial$  such that  $F \in \partial\omega_N \cap \partial T$ , one has that  $v_h|_F = v_N|_F$  so one gets using (8.2) and (8.3) that

$$\int_F |F|^{-1} k_F v_h^2 ds \lesssim k_T \sum_{M \in \mathcal{N}_F} (v_N)|_T(M) \lesssim \sum_{F' \in \partial T \setminus \{F\}} \int_{F'} |F'| k_{F'} \mu_h^2 ds.$$

By summing upon the Dirichlet sides, it follows that

$$\sum_{F \in \mathcal{F}_h^D} \int_F k_F |F|^{-1} v_h^2 ds \lesssim \|\mu_h\|_{\mathcal{M}_h}^2.$$

368 In order to obtain (8.1), we still have to establish

$$\int_{\mathcal{T}_h} K \nabla v_h \cdot \nabla v_h dx \lesssim C_K^2 \|\mu_h\|_{\mathcal{M}_h}^2. \quad (8.5)$$

369 For this purpose, we need to specify the construction of  $v_N$  at the node  $N$ , that  
 370 is to solve the system (8.4), which has a one-dimensional kernel (see [10, 21]). We fix  
 371 one of the values of  $v_N$  in order to obtain (8.5) with the best constant  $C_K$ . We recall  
 372 that  $n_N$  denotes the number of elements in  $\omega_N$  and that the cells are numbered from  
 373  $T_1$  to  $T_{n_N}$ , with  $T_1$  the element such that  $k|_{T_1} = \max_{T \subset \omega_N} k|_T$ . We suppose (without  
 374 loss of generality) that the triangles are ordered clockwise. For each  $i \in \{1, \dots, n_N\}$ ,  
 375 we set  $F_i = \partial T_i \cap \partial T_{i+1}$  with  $T_{n_N+1} = T_1$  and we recall that the sign coefficient  
 376  $\mathfrak{s}_i := \mathfrak{s}_{N, F_i}$  equals 1 if  $T_i = T^-$  with respect to  $F_i$ , and  $-1$  otherwise. For the  
 377 simplicity of notation, let us put  $v_i := (v_N)|_{T_i}(N)$  and  $\mu_i^* = \mathfrak{s}_i |F_i| \mu_h|_{F_i}(N)$ . Noting  
 378 that  $[v_N]_{F_i} = \mathfrak{s}_i (v_i - v_{i+1})$  and that  $\mathfrak{s}_i^2 = 1$ , the system (8.4) can be written as follows:

$$v_i - v_{i+1} = \mu_i^*, \quad 1 \leq i \leq n_N - 1. \quad (8.6)$$

We choose  $v_1 = 0$ . Then (8.6) yields  $v_i^2 \lesssim \sum_{j=1}^{i-1} (\mu_j^*)^2$ , for  $2 \leq i \leq n_N$ . By using that

$$\frac{1}{k_{F_j}} = \frac{1}{k_j} + \frac{1}{k_{j+1}}, \text{ we next obtain that}$$

$$k_i v_i^2 \lesssim \sum_{j=1}^{i-1} \frac{k_i}{k_{F_j}} k_{F_j} (\mu_j^*)^2 = \sum_{j=1}^{i-1} \left( \frac{k_i}{k_j} + \frac{k_i}{k_{j+1}} \right) k_{F_j} (\mu_j^*)^2, \quad 2 \leq i \leq n_N.$$

379 Recalling that  $C_N = \max_{1 \leq j \leq i \leq n_N} \frac{\sqrt{k_i}}{\sqrt{k_j}}$  on  $\omega_N$ , we have thus obtained:

$$k_i v_i^2 \lesssim C_N^2 \sum_{j=1}^{n_N-1} k_{F_j} (\mu_j^*)^2, \quad 1 \leq i \leq n_N. \quad (8.7)$$

One then has

$$\begin{aligned}
\int_{\mathcal{T}_h} K \nabla v_h \cdot \nabla v_h dx &\lesssim \sum_{T \in \mathcal{T}_h} \sum_{N \in \mathcal{N}_T} k_T (v_h)|_T^2(N) \\
&= \sum_{T \in \mathcal{T}_h} \sum_{N \in \mathcal{N}_T \cap \mathcal{N}_h^{int}} k_T (v_h)|_T^2(N) + \sum_{T \in \mathcal{T}_h} \sum_{N \in \mathcal{N}_T \cap \mathcal{N}_h^\partial} k_T (v_h)|_T^2(N) \\
&\lesssim \sum_{N \in \mathcal{N}_h^{int}} \sum_{T \in \omega_N} k_T (v_h)|_T^2(N) + \sum_{N \in \mathcal{N}_h^\partial} \sum_{T \in \omega_N} k_T (v_h)|_T^2(N).
\end{aligned}$$

Using (8.7) for the first right-hand-side term and (8.2), (8.3) for the second one, as well as the fact that  $C_N \geq 1$ , we finally get

$$\begin{aligned}
\int_{\mathcal{T}_h} K \nabla v_h \cdot \nabla v_h dx &\lesssim \sum_{N \in \mathcal{N}_h} C_N^2 \sum_{F \in \mathcal{F}_N} k_F |F|^2 \mu_h|_F^2(N) \\
&\lesssim C_\Omega^2 \sum_{F \in \mathcal{F}_h} k_F |F|^2 \sum_{N \in \mathcal{N}_F} \mu_h|_F^2(N) \simeq C_\Omega^2 \|\mu_h\|_{\mathcal{M}_h}^2
\end{aligned}$$

380 with  $C_\Omega = \max_{N \in \mathcal{N}_h^{int}} C_N$ . For  $K$  quasi-monotone, one has  $C_N = 1$  for any node  $N$  and  
381 hence,  $C_\Omega = 1$ . This ends the proof with  $\beta \simeq C_\Omega^{-1}$ .  $\square$

## REFERENCES

- 383 [1] P. Ladevèze and D. Leguillon. Error estimate procedure in the finite element method and  
384 applications. *SIAM J. Numer. Anal.*, 20(3):485–509, 1983.
- 385 [2] M. Ainsworth and J. T. Oden. A posteriori error estimation in finite element analysis. *Comput.*  
386 *Methods Appl. Mech. Eng.*, 142(1-2):1–88, 1997.
- 387 [3] L. H. Odsæter, M. F. Wheeler, T. Kvamsdal, and M. G. Larson. Postprocessing of non-  
388 conservative flux for compatibility with transport in heterogeneous media. *Comput. Meth-*  
389 *ods Appl. Mech. Eng.*, 315:799–830, 2017.
- 390 [4] P. Bastian and B. Rivière. Superconvergence and H(div) projection for discontinuous Galerkin  
391 methods. *Int. J. Numer. Methods Fluids*, 42(10):1043–1057, 2003.
- 392 [5] A. Ern, S. Nicaise, and M. Vohralík. An accurate H(div) flux reconstruction for discontinuous  
393 Galerkin approximations of elliptic problems. *C. R. Math.*, 345(12):709–712, 2007.
- 394 [6] D. Braess, V. Pillwein, and J. Schöberl. Equilibrated residual error estimates are p-robust.  
395 *Comput. Methods Appl. Mech. Eng.*, 198(13-14):1189–1197, 2009.
- 396 [7] A. Ern, A. F. Stephansen, and M. Vohralík. Guaranteed and robust discontinuous Galerkin  
397 a posteriori error estimates for convection–diffusion–reaction problems. *J. Comput. Appl.*  
398 *Math.*, 234(1):114–130, 2010.
- 399 [8] Z. Cai and S. Zhang. Robust equilibrated residual error estimator for diffusion problems:  
400 Conforming elements. *SIAM J. Numer. Anal.*, 50(1):151–170, 2012.
- 401 [9] A. Ern and M. Vohralík. Polynomial-degree-robust a posteriori estimates in a unified setting  
402 for conforming, nonconforming, discontinuous Galerkin, and mixed discretizations. *SIAM*  
403 *J. Numer. Anal.*, 53(2):1058–1081, 2015.
- 404 [10] R. Becker, D. Capatina, and R. Luce. Local flux reconstructions for standard finite element  
405 methods on triangular meshes. *SIAM J. Numer. Anal.*, 54(4):2684–2706, 2016.
- 406 [11] W. Prager and J. L. Synge. Approximations in elasticity based on the concept of function  
407 space. *Quart. Appl. Math.*, 5:286–292, 1947.
- 408 [12] L. Demkowicz and M. Swierczek. An adaptive finite element method for a class of variational  
409 inequalities. In *Proceedings of the Italian-Polish Symposium of Continuum Mechanics*,  
410 *Bologna*, 1987.
- 411 [13] J. T. Oden, L. Demkowicz, W. Rachowicz, and T. A. Westermann. Towards a universal hp  
412 adaptive finite element strategy, Part 2. A posteriori error estimation. *Comput. Methods*  
413 *Appl. Mech. Eng.*, 77(1-2):113–180, 1989.
- 414 [14] P. Destuynder and B. Métivet. Explicit error bounds in a conforming finite element method.  
415 *Math. Comput.*, 68(228):1379–1396, 1999.

- [15] M. Ainsworth and J. T. Oden. A unified approach to a posteriori error estimation using element residual methods. *Numer. Math.*, 65(1):23–50, 1993.
- [16] M. G. Larson and A. J. Niklasson. A conservative flux for the continuous Galerkin method based on discontinuous enrichment. *Calcolo*, 41(2):65–76, 2004.
- [17] T. Vejchodský. Guaranteed and locally computable a posteriori error estimate. *IMA J. Numer. Anal.*, 26(3):525–540, 2006.
- [18] D. Braess and J. Schöberl. Equilibrated residual error estimator for edge elements. *Math. Comput.*, 77(262):651–672, 2008.
- [19] R. Verfürth. A note on constant-free a posteriori error estimates. *SIAM J. Numer. Anal.*, 47(4):3180–3194, 2009.
- [20] D. Cai, Z. Cai, and S. Zhang. Robust equilibrated a posteriori error estimator for higher order finite element approximations to diffusion problems. *Numer. Math.*, 144(1):1–21, 2020.
- [21] D. Capatina and C. He. Flux recovery for Cut Finite Element Method and its application in a posteriori error estimation. *ESAIM: Math. Model. Numer. Anal.*, 55(6):2759 – 2784, 2021.
- [22] G. Matthies and L. Tobiska. Inf-sup stable non-conforming finite elements of arbitrary order on triangles. *Numer. Math.*, 102:293–309, 2005.
- [23] M. Fortin and M. Soulie. A non-conforming piecewise quadratic finite element on triangles. *Int. J. Numer. Methods Eng.*, 19(4):505–520, 1983.
- [24] R. Verfürth. A posteriori error estimation and adaptive mesh refinement techniques. *J. Comput. Appl. Math.*, 50(1-3):67–83, 1994.
- [25] A. Ern, A. F. Stephansen, and P. Zunino. A discontinuous Galerkin method with weighted averages for advection–diffusion equations with locally small and anisotropic diffusivity. *IMA J. Numer. Anal.*, 29(2):235–256, 2009.
- [26] A. Bonito, R. A. Devore, and R. H. Nochetto. Adaptive finite element methods for elliptic problems with discontinuous coefficients. *SIAM J. Numer. Anal.*, 51(6):3106–3134, 2013.
- [27] R. B. Kellogg. On the Poisson equation with intersecting interfaces. *Appl. Anal.*, 4(2):101–129, 1974.
- [28] P. Morin, R. H. Nochetto, and K. G. Siebert. Data oscillation and convergence of adaptive fem. *SIAM J. Numer. Anal.*, 38(2):466–488, 2000.
- [29] L. Demkowicz. *Computing with Hp-adaptive finite elements, Vol. 1 : One and two dimensional elliptic and Maxwell problems*. Chapman & Hall /CRC, 2007.
- [30] W. F. Mitchell. A collection of 2D elliptic problems for testing adaptive grid refinement algorithms. *Appl. Math. Comput.*, 220:350–364, 2013.